Int. J. Heat Mass Transfer. Vol. 12, pp. 863–894. Pergamon Press 1969. Printed in Great Britain

SATURATED BOILING HEAT TRANSFER IN NARROW SPACES

E. ISHIBASHI
Hitachi Research Laboratory of Hitachi Ltd., Hitachi, Ibaraki, Japan

and

K. NISHIKAWA
Mechanical Engineering Department, Kyushu University, Fukuoka, Japan

(*Received* 4 *September* 1968)

Abstract—In this study, the results of a series of experiments conducted to clarify the space restriction effect on the saturated boiling heat-transfer phenomena are reported. Through the experimental study, it was detected that the saturated boiling heat-transfer in a narrow space there is a coalesced bubble region having remarkably different characteristics beside the isolated bubble region, the heat-transfer characteristics of which have already been confirmed by many researchers. The main purpose of this study is to detect and prove the heat-transfer characteristics of the coalesced bubble region. In the first half of this study, various characteristics of the coalesced bubble region and that of the isolated bubble region are compared, based on experimental findings, and coincidently, a new type of correlating equation for the coalesced bubble region is proposed. In the last half, a theoretical analysis based on a simple unsteady-state thermal conduction model is described, and the verification to the correlating equation is demonstrated.

NOMENCLATURE

a, thermal diffusivity [m^2/h];
c, specific heat of liquid [kcal/kg'°C] (kg' denotes mass);
f_ξ, formability;
Fo, Fourier number, $= \dfrac{a}{N\Delta R^2}$;
$Fo(1)$, Fourier number based on the coalesced bubble emission frequency measured by thermocouple (1);
$Fo(c)$, Fourier number based on the coalesced bubble emission frequency at the centre height of heating surface;
$Fo(_T)$, Fourier number based on the coalesced bubble emission frequency at the upper end of heating surface;
H, total height of heating surface [m];
hi, height of point i, measured from the lower end of heating surface [m];
L, latent heat of evaporation [kcal/kg];
$N(1)$, coalesced bubble emission frequency measured by thermocouple (1) [s^{-1} or h^{-1}];
$N(i)$, coalesced bubble emission frequency at any desired point i [s^{-1} or h^{-1}];
Nu Nusselt number, $= \dfrac{\alpha . \Delta R}{\lambda}$;
$Nu(0)$, Nusselt number calculated from theoretical analysis;
p, pressure [kg/cm^2A];
Pr, Prandtl number, $= \dfrac{v}{a}$;
q, heat flux [$kcal/m^2h$];
$q(0)$, heat flux calculated from theoretical analysis [$kcal/m^2h$];
Q, equivalent heat source assumed in the liquid [$kcal/m^3h$];
ΔR, boiling space dimension [m];
Re^*, modified Reynolds number, $= \dfrac{q}{L\gamma''}\dfrac{\Delta R}{v}\left(\dfrac{q}{M_2P}\right)$

t, temperature [°C];
Δt, temperature difference between heating surface and liquid of saturated state, $= t_2 - t_1$ [°C];
t_2, temperature of heating surface [°C];
t_1, liquid temperature of saturated state [°C];
x, distance [m].

Greek symbols

α, heat-transfer coefficient [kcal/m^{2}h°C];
$\alpha(0)$, heat-transfer coefficient calculated from theoretical analysis [kcal/m^{2}h°C];
γ, specific weight [kg/m^3];
γ', specific weight of liquid [kg/m^3];
γ'', specific weight of vapour [kg/m^3];
λ, thermal conductivity [kcal/mh°C];
ν, kinematic viscosity [m^2/h];
ρ, density [kg′/m^3] (kg′ denotes mass);
σ, surface tension [kg/m];
τ, time [h].

1. INTRODUCTION

THE STUDY of boiling heat transfer is required because of its practical phase, since the field to which the boiling heat transfer is applicable is extremely wide. It is also a necessity from the phase of scientific motivation because an analysis of the phenomena has not reached a satisfactory degree. Based on this situation, research on this subject is being actively conducted on an international basis, and many research reports have been submitted. Concerning the range that the authors comprehend, however, it appears that no one has ever conducted a systematic study on the influence of the boiling space dimension upon the boiling heat-transfer phenomena. In this study, a series of experiments was conducted to ascertain the space restriction effect on the saturated-boiling heat-transfer phenomena, and the results were assembled. In the experimental apparatus for atmospheric pressure conditions, distilled water, sodium oleate aqueous solution, saponin aqueous solution, and ethyl alcohol were used as the test liquid. In the experimental apparatus for pressurized conditions, distilled water was pressurized and maintained under different levels of pressure from atmospheric pressure to 10 atg, and the saturated-boiling heat-transfer experiments were conducted in narrow spaces of various dimensions.

As the results of observing the behaviour of bubble generation when pressurized and from the various space dimensions, saturated boiling in a narrow space can be classified into an isolated bubble region (in which many small sphere bubbles are generated from the heating surface, and the bubbles depart and rise) and a coalesced bubble region (in which large coalesced bubbles are generated fully in the space, depart, and rise regularly under a low frequency).

As far as the isolated bubble region is concerned, based on the results of observation on the behaviour of bubble generation and the values of heat-transfer coefficient obtained from the experiments, it may be considered that the heat-transfer mechanism does not differ greatly in comparison with ordinary saturated pool boiling; therefore, a detailed examination was not made.

In the coalesced bubble region, the behaviour of bubble generation differs basically, in which, by comparison with the isolated bubble region, the large coalesced bubbles generate regularly under a slow cycle. The heat-transfer coefficient obtained through the experiments differs considerably from the pool boiling both quantitatively and qualitatively. This study was proceeded by placing its objective in an analysis of saturated-boiling heat-transfer mechanism in this region.

2. PROCEDURE OF EXPERIMENTS

In this study, two types of experimental apparatus were fabricated, one was for the apparatus for atmospheric pressure conditions and the other was for the apparatus for pressur-

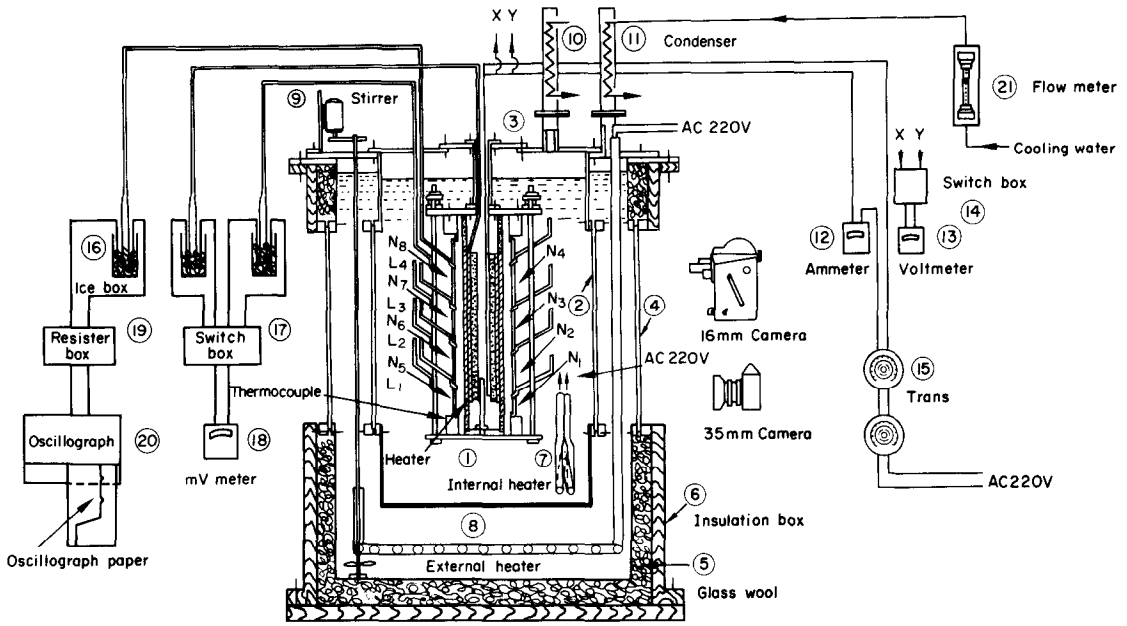

FIG. 1. Experimental apparatus for atmospheric pressure conditions.

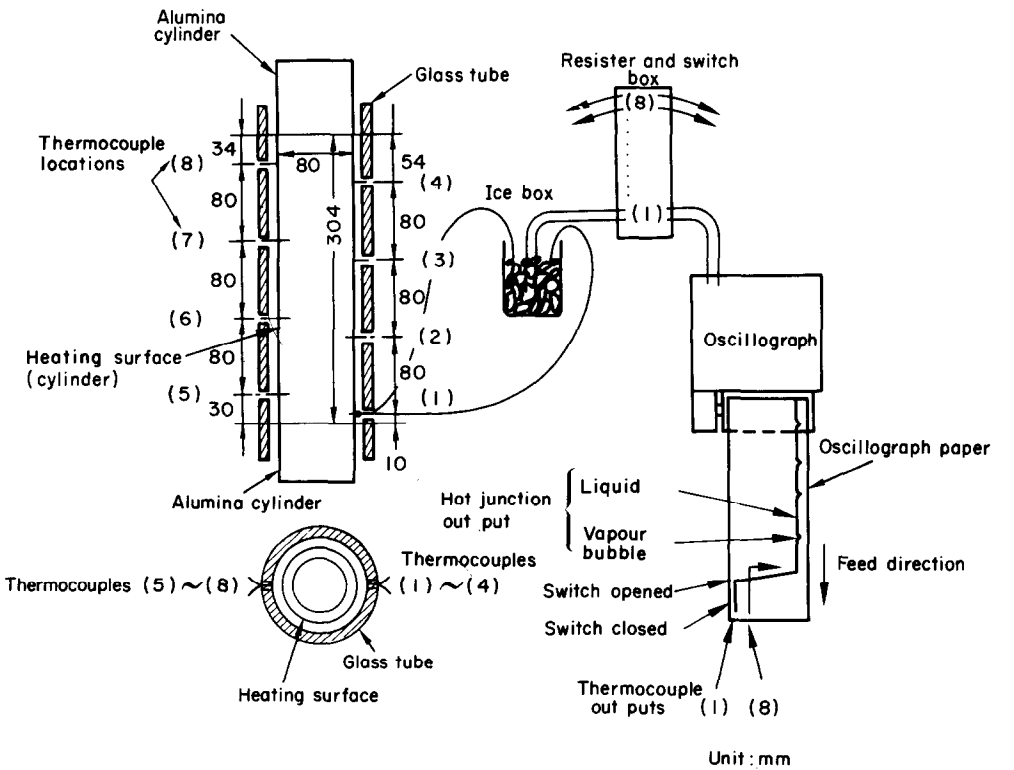

FIG. 2. Principle of coalesced bubble emission frequency measurement (atmospheric pressure conditions).

ized conditions. The difference between them was a dimensional one, but their principles were the same.

Figure 1 shows the experimental apparatus for atmospheric pressure conditions. A cylindrical heater (pure copper having an outer diameter of 80 mm and 304 mm high) was used to minimize heat loss from the heating surface. In addition, on the top and bottom ends of the heating-surface, alumina cylinders with the same outer diameter were tightly installed with packings. For measurements of the heating surface temperature, eight thermocouples were employed. The entire inner vessel containing the heating surface was placed in the outer vessel filled with distilled water of saturated temperature of the test liquid, and the outer vessel was thermally insulated with glass wool and a wooden box. Vapour generated in the inner and outer vessels was condensed by condensers (10) and (11) located on the vessels, and returned to the individual vessels respectively. Cooling water flow was adjusted so that the condensed liquid was not overcooled. A glass tube was concentrically installed on the outside of the heating surface to provide the boiling space, and by utilizing glass tubes having different inside diameters, the boiling space were changed in eight different dimensions within a range of 1 through 20 mm. Of course, experimentation was conducted without using the glass tube; in this, however, the equivalent space dimension corresponded to 82·5 mm.

In the case of atmospheric pressure water, the region became a coalesced bubble region when the boiling space dimension was approximately 3 mm or less. Thus, additional eight thermocouples and an oscillograph were used in accordance with the principle indicated in Fig. 2, and the coalesced bubble emission frequencies were measured. The thermocouples were set securely with the hot junctions projected slightly from the small holes provided on the glass tube, and temperature variations caused by the passing bubble and liquid were hourly recorded on oscillograph paper. Beside this measurement, four thermocouples were used for the measurement of bulk liquid temperature outside the glass tube.

Experimental apparatus for pressurized conditions is of a construction almost identical to that of the experimental apparatus for the atmospheric pressure conditions. However, the inner vessel was of pressure-proof construction, and the heating surface was chrome-plated in order to minimize the influence of contamination. The heating surface was a vertical cylinder made of pure copper with an outer diameter of 50 mm and 152 mm high. In a manner identical to the atmospheric-pressure apparatus, the boiling space dimension was changed in four dimensions within a range from 0·6 to 2·0 mm. Moreover, for those four dimensions, the test liquid pressure was changed in four different pressures from the atmospheric pressure to 10 atg; and thus, the experiment on saturated boiling heat transfer was conducted. The heating surface temperature, the coalesced bubble emission frequency, and the bulk liquid temperature were measured under the same procedures as for the atmospheric-pressure experiment.

The liquids used for the atmospheric-pressure experiment were distilled water, sodium oleate aqueous solution, saponin aqueous solution, and ethyl alcohol; the liquid used in the pressurized experiment was distilled water. Experiments were conducted by selecting heat flux in a proper range from 700 to 58000 kcal/m^{2}h, depending upon the type of liquids and the boiling space dimensions.

3. RESULTS OF EXPERIMENTS AND EXAMINATIONS

The saturated boiling heat transfer at a narrow space is classified into an isolated bubble region and a coalesced bubble region depending on a mutual relation between the space dimension and pressure. The individual results of the experiments are described below.

3.1 *Experiments at atmospheric pressure*

3.1.1 *Boiling behavior.* When the liquid is

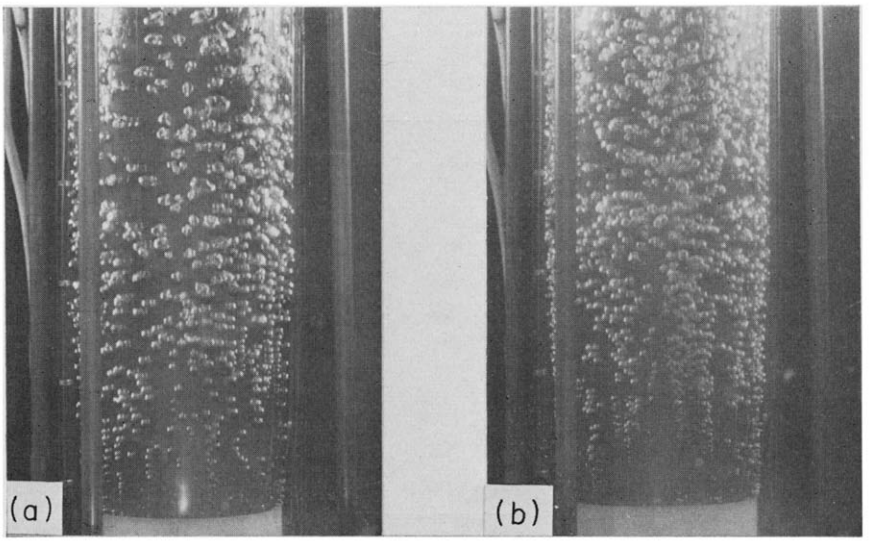

FIG. 3. Photographs of bubble generation (Isolated bubble region, atmospheric pressure water).
(a) Boiling space dimension, 5·04 mm. Liquid, distilled water, $q=40\,822$ kcal/m²h, $\alpha=6098$ kcal/m²h°C, $\Delta t=6{\cdot}70$°C
(b) Boiling space dimension, 5·04 mm. Liquid, 15 ppm sodium oleate solution, $q=40\,861$ kcal/m²h, $\alpha=6824$ kcal/m²h°C, $\Delta t=5{\cdot}99$°C

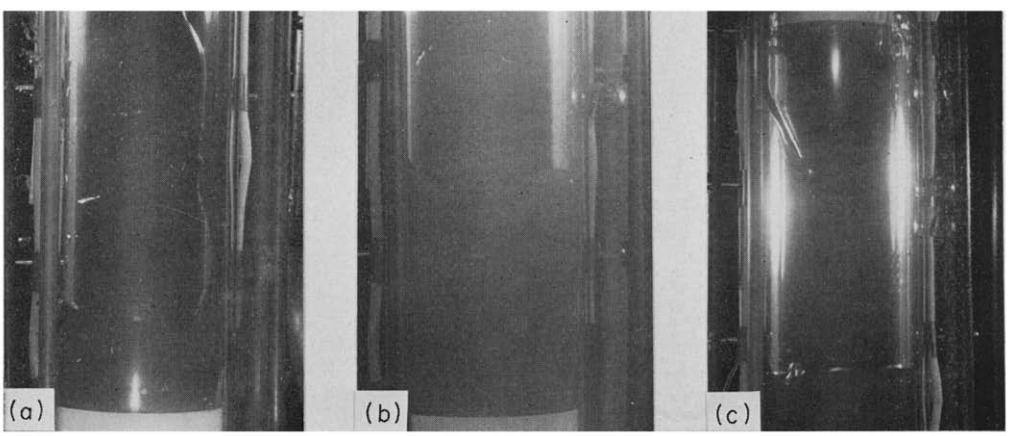

FIG. 4. Photographs of bubble generation (Coalesced bubble region, atmospheric pressure water).
(a) Boiling space dimension, 0·97 mm. Liquid, distilled water, $q=2533$ kcal/m²h, $\alpha=2360$ kcal/m²h°C, $\Delta t=1{\cdot}08$°C
(b) Boiling space dimension, 0·97 mm. Liquid, 15 ppm sodium oleate solution, $q=2497$ kcal/m²h. $\alpha=2270$ kcal/m²h°C, $\Delta t=1{\cdot}10$°C
(c) Boiling space dimension, 1·64 mm. Liquid, distilled water, $q=4569$ kcal/m²h, $\alpha=2422$ kcal/m²h°C, $\Delta t=1{\cdot}89$°C.

[*facing page* 866]

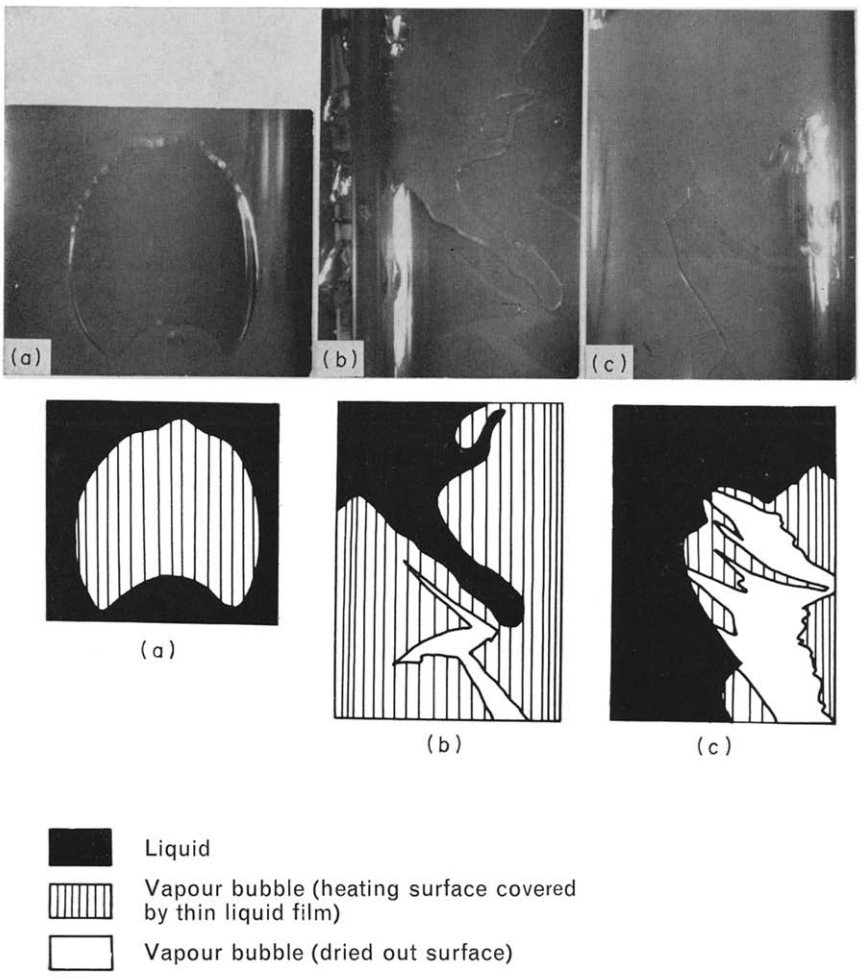

FIG. 5. Photographs of thin liquid film on the bubble bottom heating surface. Boiling space dimension, 0·97 mm. Liquid, distilled water, $q=8000$ kcal/m^{2}h, $\alpha=5300$ kcal/m^{2}h°C, $\Delta t=1{\cdot}51$ °C, $\Delta R=0{\cdot}97$ mm.

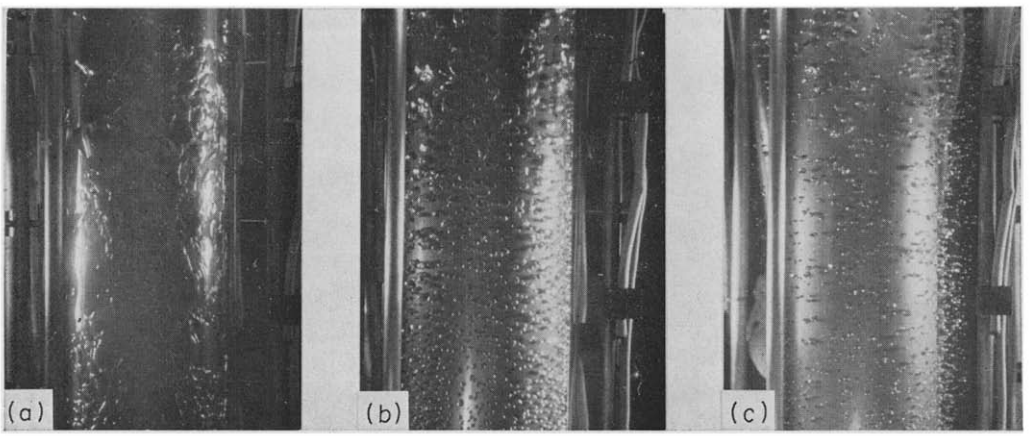

FIG. 6. Photographs of bubble generation (atmospheric pressure alcohol).
(a) Boiling space dimension, 0·97 mm. Liquid, ethyl alcohol. Region, coalesced bubble region, $q=8522$ kcal/m²h, $\alpha=3312$ kcal/m²h°C, $\Delta t=2{\cdot}58$°C.
(b) Boiling space dimension, 2·36 mm. Liquid, ethyl alcohol. Region, isolated bubble region, $q=8071$ kcal/m²h, $\alpha=1424$ kcal/m²h°C, $\Delta t=5{\cdot}67$°C.
(c) Boiling space dimension, 82·5 mm. Liquid, ethyl alcohol. Region, isolated bubble region, $q=7863$ kcal/m²h, $\alpha=861$ kcal/m²h°C, $\Delta t=9{\cdot}14$°C.

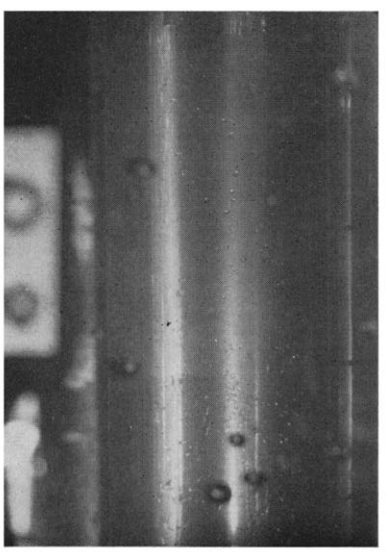

FIG. 7. Photograph of heating surface at liquid deficient region.
Boiling space dimension, 0·57 mm. Liquid, distilled water, $p=1{\cdot}03$ata $q=79261$ kcal/m²h, $\alpha=3666$ kcal/m²h°C, $\Delta t=21{\cdot}62$°C.

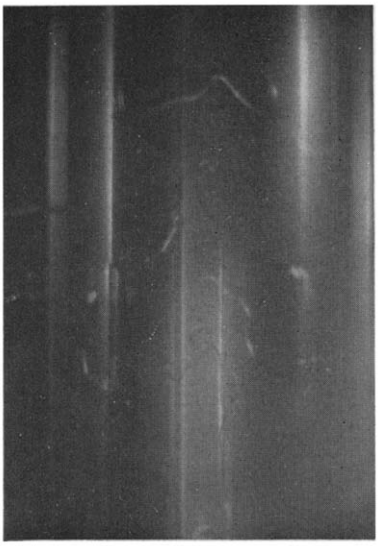

FIG. 19. Photograph of coalesced bubble generation in case of pressurized water.
Boiling space dimension, 0·57 mm. Liquid, distilled water, $p=4{\cdot}16$ ata $q=43\,972$ kcal/m^{2}h, $\alpha=13365$ kcal/m^{2}h°C, $\Delta t=3{\cdot}29$°C.

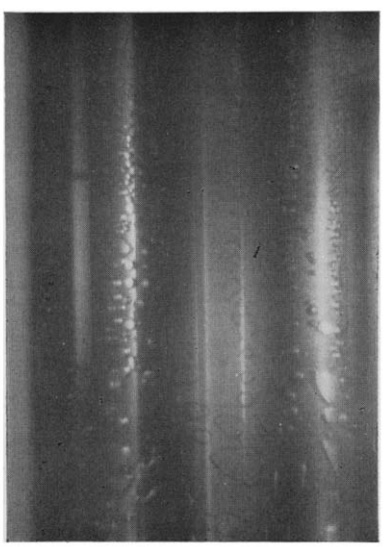

FIG. 20. Photograph of isolated bubble generation in case of pressurized water.
Boiling space dimension, 0·57 mm. Liquid, distilled water, $p=11{\cdot}28$ ata $q=30\,745$ kcal/m^{2}h, $\alpha=11044$ kcal/$\Delta t=2{\cdot}78$°C.

distilled water of atmospheric pressure, and the space is approximately 3 mm or more, many small sphere bubbles generated from the heating surface are observable. Diameters of bubbles at the centre of the heating surface were 3–3·5 mm on an average in the case of saturated pool boiling (equivalent space dimension: 8·25 mm), and in the case of a space dimension of 5·04 mm, only the increase of bubble rising velocity is externally visible and no significant change is apparent. Under the same space dimension and heat flux, bubbles of sodium oleate aqueous solution having small surface tension are slightly smaller than those of the distilled water. Figure 3 shows typical behaviour of bubble generation in the isolated bubble region.

When the space dimension is smaller than approximately 3 mm, no isolated bubble generation can be observed, but large coalesced bubbles are generated within the space (as shown in Fig. 4), and the behaviour becomes quite different from that of the isolated bubble region described above. For example, the size of one of these coalesced bubbles reaches a height of approximately 300 mm when the space dimension is 0·97 mm, and then the entire heating surface is completely covered by the bubble momentarily. These coalesced bubbles are regularly generated one after another in the space, under a slow cycle. When coalesced bubbles are generated, the existence of a thin liquid film on the heating surface occupied by the bubble is visible. Figure 5 shows a series of photographs taken at a close-up position to the occupied surface when distilled water is saturate-boiled under a heat flux of approximately 8000 kcal/m^{2}h, within a space of 0·97 mm. Figure 5(a) shows the condition immediately after generation of the bubble. Liquid in the upper part of the vapour bubble is displaced by the expanding bubbles, and the vapour bubble interface assumes a crater shape. At the lower part, the buoyancy force and the expansion force are balanced, and a smooth vapour liquid interface is observable. The thin liquid film on the occupied surface still exists. Figure 5(b) shows the condition at the time when it elasped a small time interval after the generation of bubble. Part of the thin film has evaporated, the heating surface is exposed, and a colour differing from that of the surrounding thin film parts, that is, the white tone can be seen. Figure 5(c) shows the thin film, the majority of which is dried out, and the dried-up area becomes wet again due to the rising liquid. As the result of visual observation over a long period, it seems that the shapes of this dried-up area are not constant and is not reproducible.

Also when alcohol is saturate-boiled in a narrow space, in a manner identical to distilled water, the region may also be classified into an isolated bubble region and a coalesced bubble region. In this case, however, the coalesced bubble region occurs only when the space dimension is 0·97 mm (differing from distilled water); and at a space dimension of 1·64 mm or greater, isolated bubbles are generated. Figure 6 shows the behaviour of bubble generation at various space dimensions.

When the space dimension is extremely small, when the space dimension is small and heat flux is comparatively high, or when the pressure of

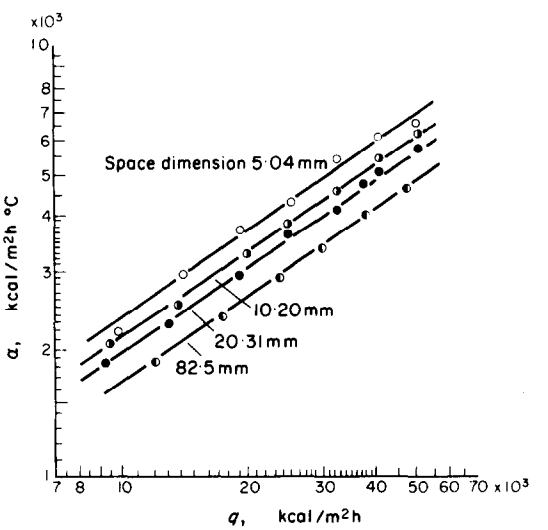

FIG. 8. Relation among heat-transfer coefficient, heat flux and boiling space dimension (atmospheric pressure water, isolated bubble region).

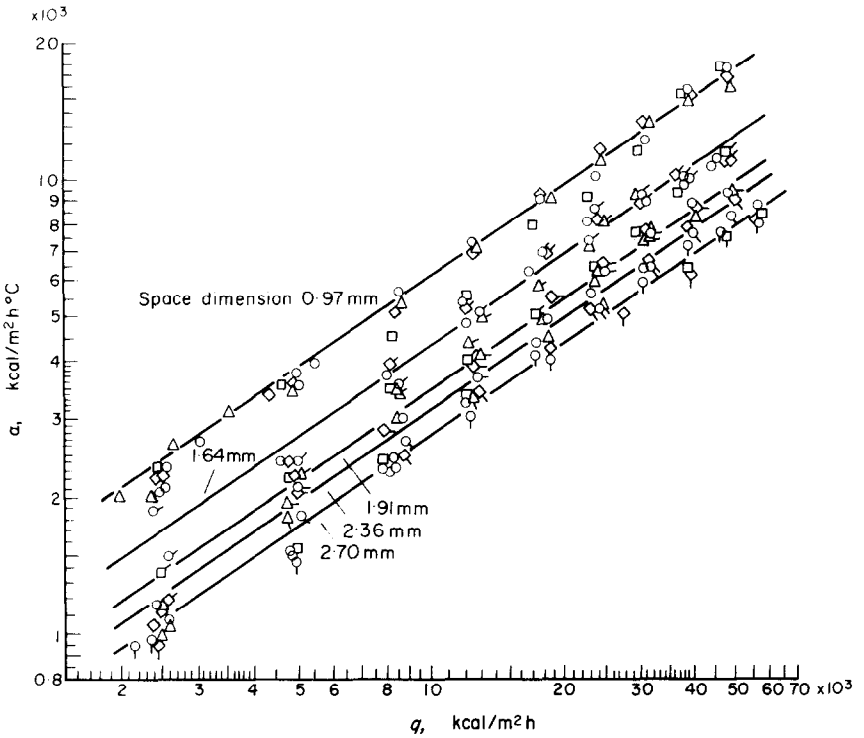

Symbol	Space mm	Liquid	Symbol	Space mm	Liquid
○	0·97	Distilled water	◇	0·97	15 ppm sodium oleate
○	1·64	Distilled water	◇	1·64	15 ppm sodium oleate
○	1·91	Distilled water	◇	1·91	15 ppm sodium oleate
○	2·36	Distilled water	◇	2·36	15 ppm sodium oleate
○	2·70	Distilled water	◇	2·70	15 ppm sodium oleate
△	0·97	3 ppm sodium oleate	□	0·97	400 ppm saponin
△	1·64	3 ppm sodium oleate	□	1·64	400 ppm saponin
△	1·91	3 ppm sodium oleate	□	2·70	400 ppm saponin
△	2·36	3 ppm sodium oleate			
△	2·70	3 ppm sodium oleate			

FIG. 9. Relation among heat-transfer coefficient, heat flux and boiling space dimension (atmospheric pressure water, coalesced bubble region).

test liquid is low, phenomena occur different from those described above. Namely, at the beginning, generation of a coalesced bubble is seen in the boiling space; however, as time passes, the space volume occupied by vapour gradually increases in comparison to that by the liquid. The ring-shaped liquid band existing between the coalesced bubbles is eliminated, and liquid in the considerable numbers of small droplets adhere to the heating surface and glass

tube interior. These droplets actively continue to evaporate within a small restricted range, and fade out gradually.

Hereinafter, the region in which this dryout phenomenon proceeds on the heating surface is called the liquid deficidnt region. Figure 7 is an external view of the heating surface in the liquid deficient region.

3.1.2 *Heat transfer.* (a) Isolated bubble region.

Figure 8 shows the relation between heat flux and heat-transfer coefficient of distilled water in the isolated bubble region.

$$\alpha \propto q^{\frac{1}{3}}. \tag{1}$$

When heat flux is identical, the smaller the space, the more the heat-transfer coefficient increases, and when giving consideration to the influence of space dimensions, the following equation can be established:

$$\alpha \propto q^{\frac{1}{3}} \Delta R^{-0.13}. \tag{2}$$

It corresponds to formability $f_\xi = 1{\cdot}33$ at Nishikawa's equation [1] $\alpha = 3{\cdot}16\, q^{\frac{1}{3}} f_\xi^{\frac{1}{3}}$ which is a correlating equation of boiling heat transfer in the case of pool boiling of distilled water. Further, for the influence of the surface tension, Jakob's method [2] will be applied.

Although the influence is comparatively small in the isolated bubble region, the heat-transfer coefficient increases more and more at the constant heat flux, as the space reduces.

Thus, considering that the cause for this is a forced convection effect due to natural circulation of liquid within the boiling space and the apparatus, tentative examinations were conducted by the following two methods:

(i) Method in which heat-transfer coefficient is obtained by an empirical equation by Piret and Isbin [3].

(ii) Clark–Rohsenow's method in which total heat flux is obtained as a sum of heat flux due to single-phase forced convection and pool boiling heat flux.

However, with these methods, the influence of the space dimensions could not be explained. For this reason, it is assumed that the tendency of heat-transfer coefficient due to boiling space dimensions at an isolated bubble region must obtain its factor somewhere else other than the forced convection effect. It is considered that the behaviour of bubble generation and the stirring effect of bubbles in a narrow space differ from those in pool boiling, even in the range where isolated bubbles generate.

(b) Coalesced bubble region. Also at the coalesced bubble region which indicates quite a different behaviour of bubble generation than that at the isolated bubble region, the relation between heat-transfer coefficient and heat flux is expressed by the equation (1). Figure 9 indicates the relation between the heat-transfer coefficient and heat flux at the coalesced bubble region. In the coalesced bubble region, the heat-transfer coefficient remarkably increases when the heat flux is the same, in comparison with the isolated bubble region. For example, when the space dimension is 0·97 mm, the heat-transfer coefficient is approximately 3·8 times as great as that in pool boiling. Further, separation of the α–q curves, caused from a difference in surface tension which was seen in the isolated bubble region, cannot be observed. Also, regarding the sodium oleate aqueous solution of 15 ppm, the surface tension of which is 14 per cent smaller than that of distilled water, the same relation as that for the distilled water can be established. It can be said that the elimination of the influence of surface tension on the heat-transfer coefficient is one of major characteristics in the coalesced bubble region. This indicates that the bubbles are squeezed within a narrow space, and regardless of surface tension, the behaviour of the generated bubbles is regulated by the heat flux and the space dimension. It is assumed that the effect of generated bubbles which affects the heat-transfer mechanism quite differs from that of an isolated bubble.

In the coalesced bubble region, a remarkable increase of heat-transfer coefficient can be seen in comparison with the isolated bubble region. However, when comparing the heat flux at a

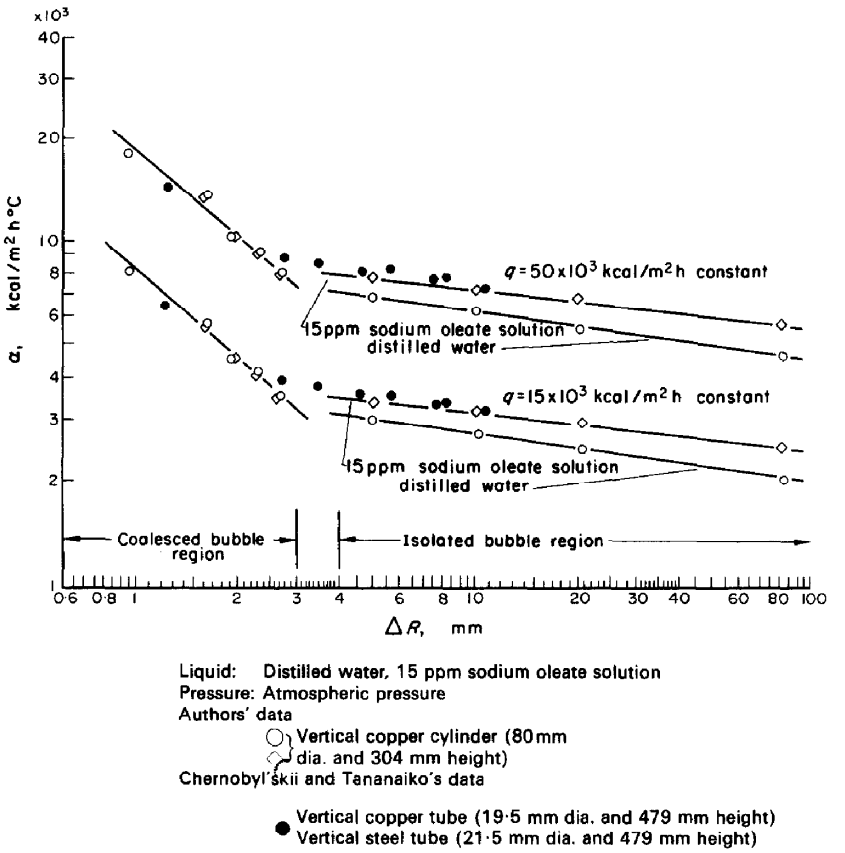

FIG. 10. Variation of heat-transfer coefficients due to change of boiling space dimensions (atmospheric pressure water, constant heat flux).

constant temperature difference, this tendency is more emphasized. The relations between the heat flux and temperature difference at the isolated bubble region and coalesced bubble region are expressed by the following equation:

$$q \propto \Delta t^3. \tag{3}$$

The proportional constant of the above equation at the same heat flux becomes approximately 32 times as great as that in the case of pool boiling when the space dimension is 0·97 mm.

In the coalesced bubble region, as well as that of the isolated bubble region, the smaller the space dimension at the same heat flux, the more the heat-transfer coefficient increases. However, the influence of a change in space dimension also increases, and is expressed by the following equation:

$$\alpha \propto q^{\frac{1}{3}} \Delta R^{-\frac{1}{3}} \tag{4}$$

Moreover, in order to comprehend changes in the heat-transfer coefficient due to space dimensions more clearly, the relations of $\alpha - \Delta R$ with a constant heat flux under $q = 50{,}000$ kcal/m^{2}h and $q = 25{,}000$ kcal/m^{2}h were obtained. This relation is shown in Fig. 10. In this figure, the experimental points established by Chernobyl"skii and other are also plotted. The experimental points of the coalesced bubble region

indicate an extremely satisfactory agreement against the result of this experiment both quantitatively and qualitatively. However, the experimental points of the isolated bubble region indicate a slight deviation quantitatively but are completely in agreement qualitatively, and equation (2)—the result of this experiment—is satisfied.

the ripples corresponds to the liquid passing time.

As described previously, thermocouples (1) and (5) are set approximately at the same height, making a 180° angle between them. However, based on the fact that the ripples of both thermocouples are timely in agreement, it is assumed that the bubbles generated in the space

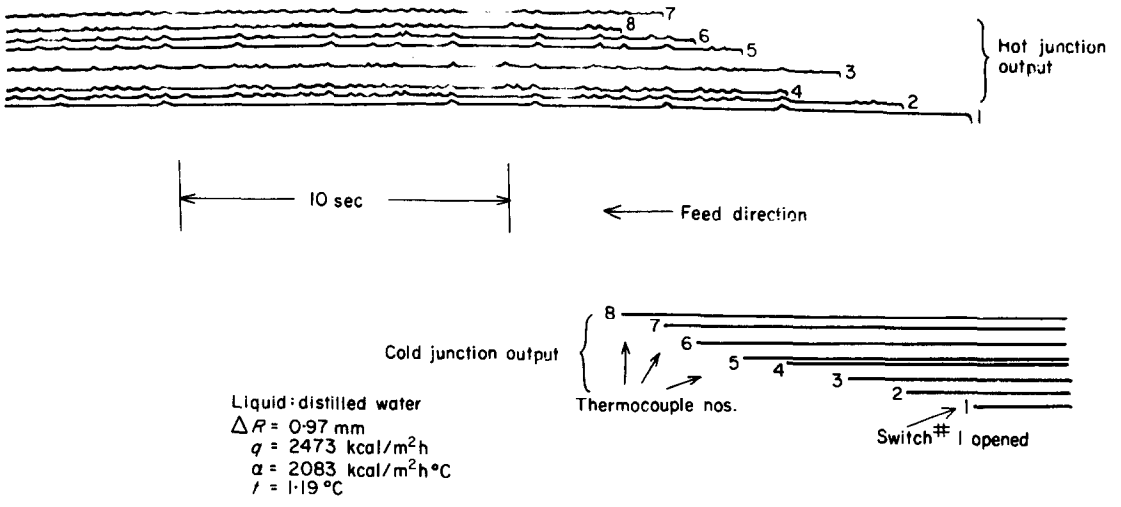

FIG. 11. A typical oscillographic record of coalesced bubble emission (atmospheric pressure water).

Figure 11 is a section of a typical record on which bubble emission frequency was measured in the coalesced bubble region on oscillograph paper, in accordance with the instrumentation indicated in Fig. 2. The horizontal axis indicates the time (time proceeds from right to left), and the vertical axis indicates the telperature.

The horizontal lines at the right, lower end indicate the outputs generated when the thermocouple outputs were short-circuited by switches. These lines indicate the cold junction outputs (i.e. 0°C). When the switches are opened, temperature changes of the hot junctions are recorded as horizontal lines including ripples on the upper part. These ripples indicate bubble passing times, and the straight line part between

grow rapidly in all directions, form a continuous bubble band around the heating surface, and displace the liquid in the space. It is assumed that the reason why the number of ripples increases as the measuring point rises is because of the increase of the bubble generating sites at the higher side of the heating surface. The emission frequency which would be considered to be the representative bubble emission frequency is described in the subsequent paragraph.

Figure 12 indicates the relation between coalesced bubble emission frequency and heat flux. The value actually measured by thermocouple (1) was used for the coalesced bubble emission frequency in this case. As can be understood from this figure, the coalesced

bubble emission frequency becomes proportional to the heat flux, when the space dimension is constant. In other words, the following equation can be established:

$$N_{(1)} \propto q. \tag{5}$$

region. The coalesced bubble emission frequency is in relation to heat flux and space dimensions, not in relation to surface tension, and the following equation can therefore be established:

$$N_{(1)} \propto q\,\Delta R^{-\frac{1}{2}}. \tag{6}$$

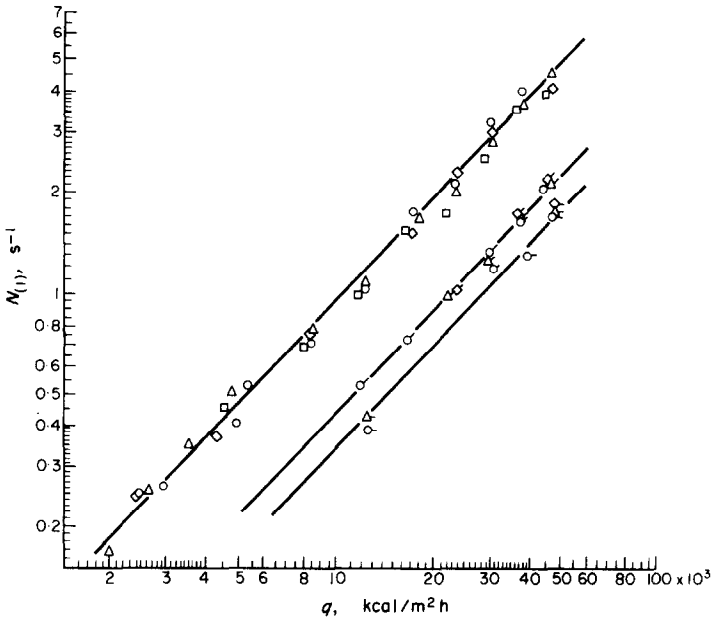

Symbol	Space mm	Liquid
○	0·97	Distilled water
○	1·64	Distilled water
○	1·91	Distilled water
△	0·97	3 ppm sodium oleate
△	1·64	3 ppm sodium oleate
△	1·91	3 ppm sodium oleate
◇	0·97	15 ppm sodium oleate
◇	1·64	15 ppm sodium oleate
◇	1·91	15 ppm sodium oleate
□	0·97	400 ppm saponin

FIG. 12. Relation among coalesced bubble emission frequency, heat flux and boiling space dimension (atmospheric pressure water).

As is obvious from Figure 12, there is no influence of surface tension for the $N_{(1)}$–q relation. As described above, this agrees with the fact that there is no influence of surface tension for α–q relation in the coalesced bubble

Figure 13 indicates the relation between the coalesced bubble emission frequency and heat flux when alcohol is saturate-boiled within a narrow space of 0·97 mm, by comparing it with that of the distilled water. Also in alcohol, the

physical properties of which remarkably differ from those of water, the coalesced bubble emission frequency becomes proportional to the heat flux under a comparatively low heat flux or even less (in this case, approximately heat-transfer coefficient and heat flux differs considerably from the equation (1), and the following equation is established:

$$\alpha \propto q^{0.12}. \tag{7}$$

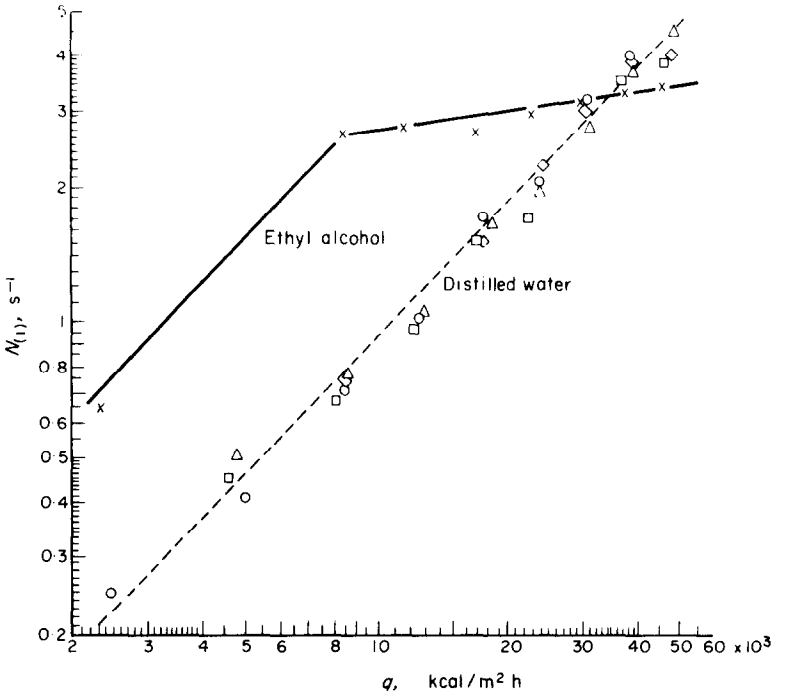

Symbol	Space mm	Liquid
—○—	0·97	Distilled water
— △—	0·97	3 ppm sodium oleate
—◇—	0·97	15 ppm sodium oleate
—□—	0·97	400 ppm saponin
— × —	0·97	Ethyl alcohol

FIG. 13. Relation between coalesced bubble emission frequency and heat flux (atmospheric pressure alcohol and water, boiling space dimension at 0·97 mm).

8000 kcal/m^{2}h), and the establishment of equation (5) can be recognized. At a heat flux above that level, the emission frequency becomes far smaller than that expressed by equation (5). In this region, however, the relation between the

When endeavouring to describe this region as the pre-burnout region that is directly connected with burnout, it was found that the heat-transfer coefficient of this region could be correlated with the coalesced bubble emission

frequency in a manner identical to that at the normal coalesced bubble region. This fact indicates that the coalesced bubble emission frequency controls the boiling heat-transfer mechanism also in this region.

to the heat flux at the individual measuring points, and further, the higher the measuring point is, the larger frequency becomes through a certain rule at the same heat flux, and parallel line groups separated by the measuring points

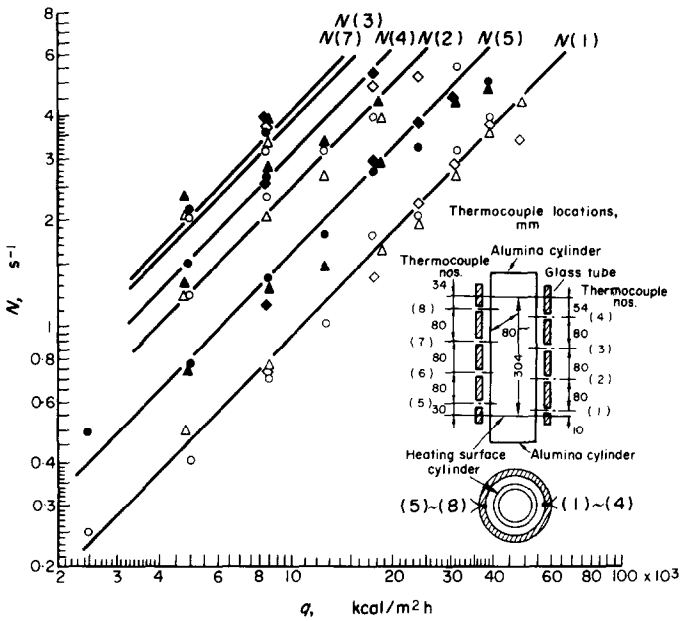

Symbol	Space mm	Press ata	Liquid
○●	0·97	1·03	Distilled water
△▲	0·97	1·03	3 ppm sodium oleate
◇◆	0·97	1·03	15 ppm sodium oleate

FIG. 14. Relation between coalesced bubble emission frequency and heat flux at different height of heating surface (atmospheric pressure water, boiling space dimension at 0·97 mm).

Now, since the coalesced bubble emission frequency was measured by the eight thermocouples installed at different heights, change of the frequency at the heating surface height direction could be determined. Figure 14 indicates these relations for a space dimension of 0·97 mm. As the frequency becomes proportional

can be obtained. These frequencies can be correlated to one line by the following experimental equation in which the influence of height is considered:

$$N_{(i)} \propto q\left(\frac{h_i}{H}\right)^{\frac{1}{4}}. \qquad (8)$$

Here, $N_{(i)}$ is a coalesced bubble emission frequency at any desired height "i".

When determining which point on the heating surface should be used for the representative coalesced bubble emission frequency, any one of the points can be fixed and the frequency at this point may be used qualitatively. Thus, it was decided to use the frequency $N_{(1)}$ measured by thermocouple (1) as a representative value with which a perspicious value can be obtained for wider heat flux ranges. Moreover, in the forthcoming examination, value at the upper end of the heating surface may also be used as the meaning of total emission frequency.

Next, vapour temperature within the coalesced bubble is described. From the ripple shape shown in the Fig. 11, it is understandable that the vapour in the bubble is superheated by approximately 1°C higher than that of the surrounding liquid. This superheat degree is not related to the heat flux, or space dimension; further, it

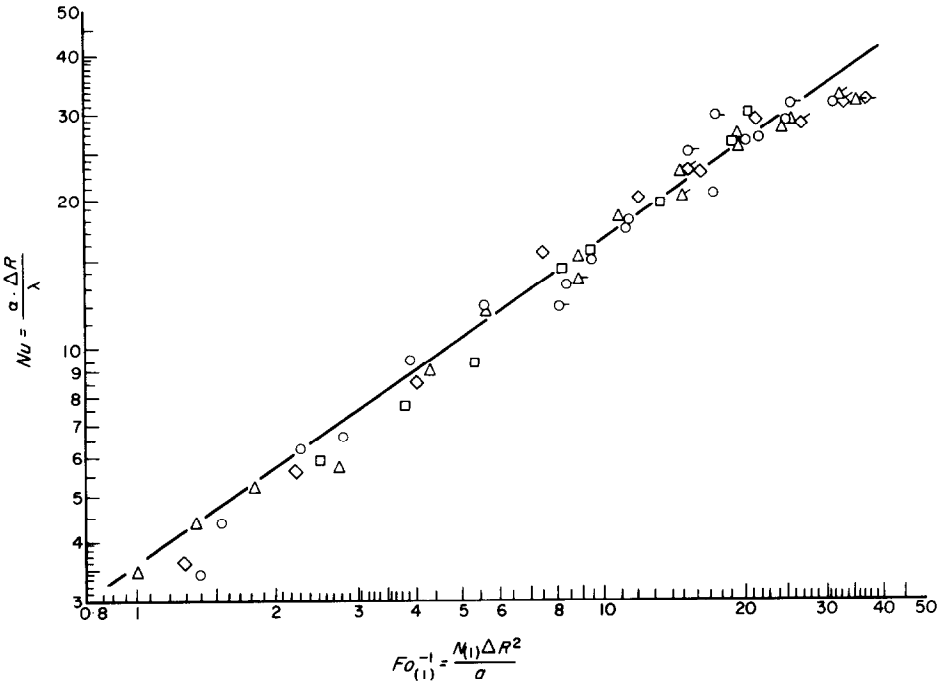

Symbol	Space mm	Liquid	Symbol	Space mm	Liquid
○	0·97	Distilled water	◇	0·97	15 ppm sodium oleate
○	1·64	Distilled water	◇	1·64	15 ppm sodium oleate
○	1·91	Distilled water	◇	1·91	15 ppm sodium oleate
△	0·97	3 ppm sodium oleate	□	0·97	400 ppm saponin
△	1·64	3 ppm sodium oleate			
△	1·91	3 ppm sodium oleate			

FIG. 15. Correlation of heat-transfer coefficients in coalesced bubble region by $Nu \sim Fo^{-1}$ (atmospheric pressure water).

seems that there is no influence from height of the heating surface.

Conventionally, regarding the growth of the bubble on the horizontal heating surface, using the Schlieren method, it has been confirmed that the generated bubble raises the superheated liquid layer, and it has been assumed that mass and heat transfer from this superheated layer into the bubble is one of the main factors of the bubble growth [7, 8]. Moreover, the same idea also applies to the growth of bubbles in the coalesced bubble region in a horizontal narrow space [9]. However, concerning the bubbles in the coalesced bubble region there is no such superheated layer which encircles the bubbles, and mass and heat-transfer processes from the surrounding liquid into the bubbles do not occur, as shown from the above-described experimental fact. Based on this fact, it is assumed that a thin liquid film exists on the heating surface at the bubble bottom, and a part of the generated heat flows into the bubble through this film (existence of this thin film has already been shown in Fig. 5).

It is considered that the heat-transfer mechanism at the coalesced bubble region is due to periodical displacement of the liquid with the bubbles based on the result of observation of bubble generating behaviour. Hence, the coalesced bubble emission frequency becomes the main factor which manages the heat transfer in this region. Based on this fact, taking the Nusselt number and Fourier number respectively on the coordinates, and the experimental values for the atmospheric pressure water were correlated with a single line as shown in Fig. 15. And the following equation is established.

$$Nu = 3{\cdot}45\, Fo_{(1)}^{-\frac{3}{2}}. \qquad (9)$$

Next, when calculating the rate of latent heat transport of the bubbles, it becomes approximately 9 per cent of the total heat flux at the space dimension of 0·97 mm. It is assumed that the remaining heat energy is accumulated within the boundary layer of the liquid, and after being torn off forcibly by the bubbles generated over almost the entire periphery of the space, the superheated liquid in the space, is pushed up into the bulk liquid, evaporated, and diffused.

The heat-transfer coefficient at the coalesced bubble region is increased by the forced tearing off of the boundary layer due to the bubbles, and it can be said that the bubble emission frequency controls the time rate of tearing off (the heat-transfer coefficient). Moreover, at the narrow space of isolated bubble region, the heat-transfer coefficient increases slightly in comparison with pool boiling; however, its increasing rate is not as great as that in the coalesced bubble region. It is considered that this is because the heat is transferred by the boundary layer stirring by the bubbles as in ordinary pool boiling, and the tearing off of the boundary layer by the bubbles is not predominate and is not the major controlling factor.

Now, the result of the experiment by Chernobyl'skii and other [5] is examined. They conducted an atmospheric-pressure experiment of saturated boiling heat transfer at narrow spaces down to the minimum space of 1·25 mm, and reported as follows.

"The cause of the increase of heat-transfer coefficient in narrow space can be understood from the visual observations conducted by ourselves and by other investigators, which showed that with reduced slit width the character of vapour formation is changed: the size of the vapour bubbles is reduced, the turbulence of the flow is increased and the overall vapour content of the mixture rises. The trajectories of the small vapour bubbles are transferred to the periphery and the liquid is violently agitated: this leads to a high rate of heat removal from the heated wall, the wall temperature drops and the heat-transfer coefficient is increased. Visual observations were performed for slits of four sizes: δ = 14 mm to 3·5 mm."

The results of their experiment entirely differ from the observation results of bubble generating behaviour of the coalesced bubble region in this study. However, the minimum space dimension in which they conducted the

observation of the bubble generating behaviour was 3·5 mm. According to detailed observation results of bubble generation in this study, it does not belong in the coalesced bubble region under saturated boiling of atmospheric-pressure water when the space dimension is 3·5 mm. Hence, we assume that their conclusion was made by extending the influence of the space dimensions on the bubble generating behaviours simply at an isolated bubble region without observing the particular bubble generating behaviour in the coalesced bubble region.

abscisa, it becomes as shown in Fig. 16. All experimental points are aligned on one line, and the following equation can be established:

$$Nu = 13{\cdot}6\{Re^{*\frac{1}{2}}\}^{\frac{3}{4}} \tag{10}$$

Experimental results in the cases of space dimensions of 1·25 and 2·75 mm by Chernobyl'skii and other [5], which are considered belonging to the coalesced bubble region are also calculated and plotted. However, these values are reasonably aligned by the equation (10) in this figure.

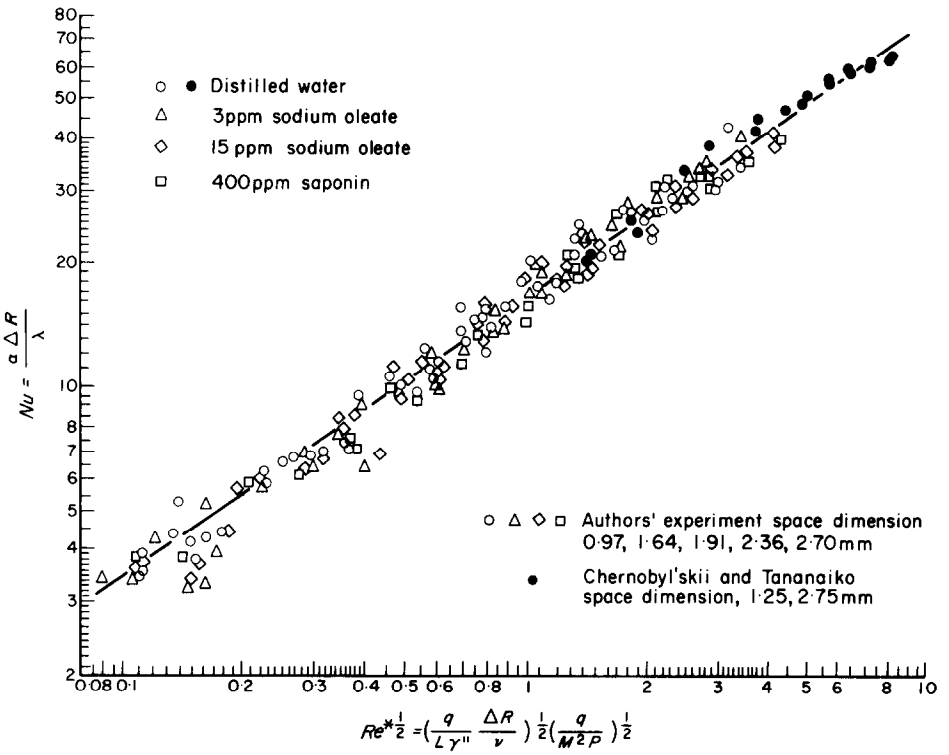

FIG. 16. Correlation of heat-transfer coefficients in coalesced bubble region by $Nu \sim Re^{*\frac{1}{2}}$ (atmospheric pressure water).

The coalesced bubble emission frequency is regulated by the heat flux and space dimension; therefore, in order to correlate those data by taking the Nusselt number on the ordinate and the root of the modified Reynolds number "$Re^{*\frac{1}{2}}$" (used in the Nishikawa's correlating equation for boiling heat transfer [1]) on the

In the above, experimental data pertaining to the atmospheric-pressure water was described. In the following, experimental data on the atmospheric-pressure alcohol is described and correlated. As is indicated in the case of atmospheric-pressure water, there are two correlating methods of heat-transfer coefficient at

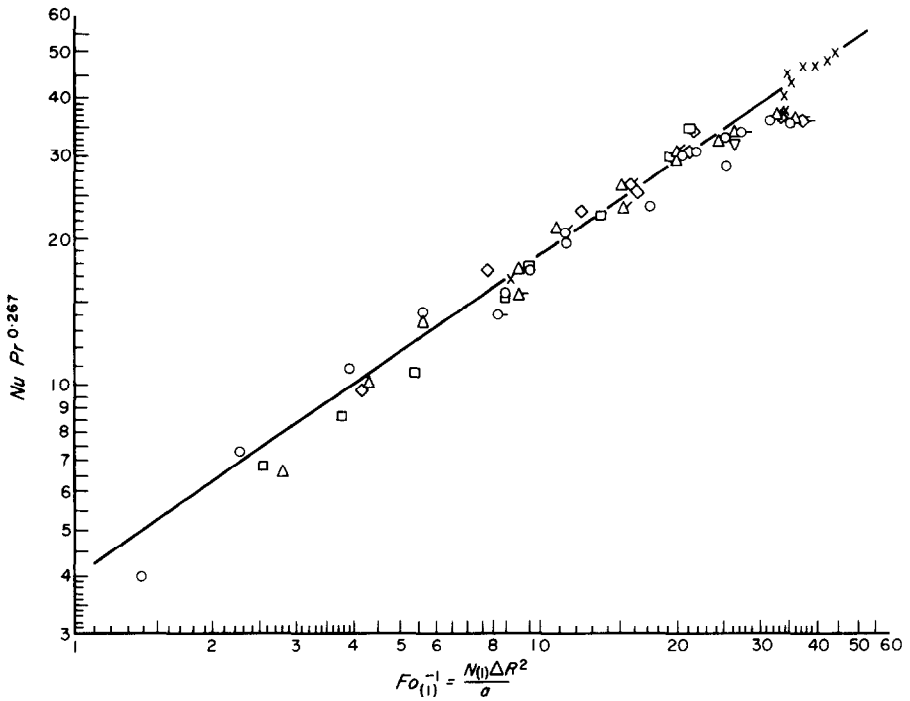

Symbol	Space mm	Press. ata	Liquid	Symbol	Space mm	Press. ata	Liquid
○	0·97	1	Distilled water	◇	0·97	1	15 ppm sodium oleate
○–	1·64	1	Distilled water	◇/	1·64	1	15 ppm sodium oleate
○/	1·91	1	Distilled water	◇–	1·91	1	15 ppm sodium oleate
△	0·97	1	3 ppm sodium oleate	□	0·97	1	400 ppm saponin
△/	1·64	1	3 ppm sodium oleate				
△–	1·91	1	3 ppm sodium oleate	×	0·97	1	Ethyl alcohol

FIG. 17. Correlation of heat-transfer coefficients in coalesced bubble region by $NuPr \sim Fo^{-1}$ (atmospheric pressure water and alcohol).

the coalesced bubble region—one is the *Nu–Fo* correlating method and the other is the *Nu–Re** correlating method. By applying these two methods to the experimental values of alcohol, the correlating methods are now compared and examined.

With the *Nu–Re** correlating method, the experimental points of normal coalesced bubble region can be correlated. However, the experimental points in the pre-burnout region could not be correlated. According to the *Nu–Fo* correlating method, the experimental points of the entire heat flux range (including the pre-burnout region) can be correlated by the

following equation as shown in Fig. 17.

$$Nu = 4{\cdot}00\, Fo_{(1)}^{-\frac{3}{4}} Pr^{-0{\cdot}267}. \quad (11)$$

Now, these two correlating methods are simply compared and examined. Advantages of the *Nu–Re** correlating method are that the heat-transfer coefficient can be obtained without using the coalesced bubble emission frequency by taking only the space dimension for the in the coalesced bubble region. However, there is still a problem in that the coalesced bubble emission frequency which must be obtained by experiment is required.

(c) Liquid deficient region.

Figure 18 indicates relation between the heat-transfer coefficient and heat flux during saturated boiling at atmospheric pressure when the space dimension was 0·57 mm. In the normal boiling range of heat flux, $q < 8500$ kcal/m^{2}h, the relation between heat-transfer coefficient and

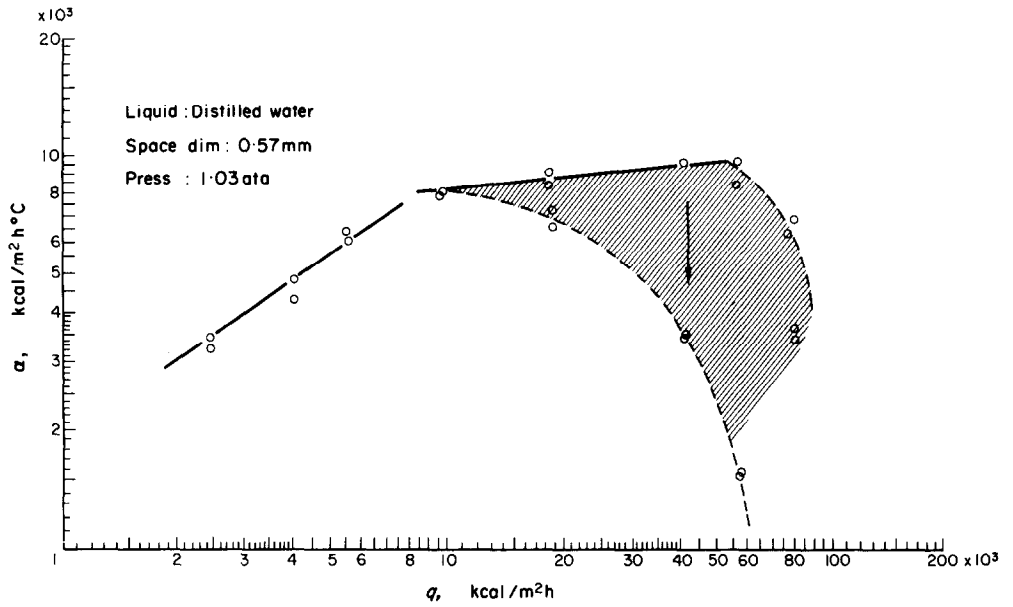

FIG. 18. Relation between heat-transfer coefficient and heat flux at 0·97 mm boiling space (atmospheric pressure water, coalesced bubble region and liquid deficient region).

representative length. However, with this method, the experimental points of the pre-burnout region cannot be correlated. On the other hand, in the *Nu–Fo* correlating method the space dimension is taken for the representative length, and further, the Fourier number based on the bubble generating frequency is used. By this method, experimental points at both the normal coalesced bubble region and pre-burnout region can be correlated. Thus, it can be said that the *Nu–Fo* correlating method is more essential for the heat-transfer mechanism heat flux is expressed by equation (1). In this case, large coalesced bubbles are generated, rising regularly within the narrow space under a low frequency, and on the heating surface occupied by the bubble, the existence of a thin film of liquid is visible. The coalesced bubble emission frequency becomes proportional to the heat flux, equation (5) is established, and the heat-transfer characteristics are regulated by the space dimension.

In a range of heat flux, $q = 8500$ to 50000 kcal/m^{2}h, the increasing rate of heat-transfer

coefficient by the increase of heat flux becomes extremely small, and the pre-burnout which was seen in the alcohol appears. The relation between heat flux and heat-transfer coefficient in this region can be expressed by equation (7). When the heat flux is increased from the heat flux before the pre-burnout to the heat flux in which this phenomenon appears, boiling space behaviour is such that the generation of the coalesced bubbles is initially visible. However, shortly afterward the generation frequency lowers rapidly and settles at a certain value. The behaviour at this time is the condition in which equation (7) is established. The vigorous coalesced bubble generation, observable immediately after the increase of heat flux, tends to increase the frequency to the value indicated by equation (5) in response to the heat flux. However, due to the increase of flow resistance by the bubbles generated in the space, this tendency is depressed, and it is assumed that the behaviour settles a stationary state as indicated by equation (7). For this reason, it is assumed that, up to this heat flux range, the main factor which manages the boiling heat-transfer mechanism is the coalesced bubble emission frequency.

Next, we will describe the time-dependent characteristics of the heat-transfer coefficient at the pre-burnout region. When the condition in which equation (7) is established (an apparent stationary state) is left for a long period under the constant heat flux, the heating surface temperature indicates a gradual rise; and the heat-transfer coefficient gradually reduces (as indicated by the arrow mark in Fig. 18). More specifically, the heat-transfer coefficient in this region becomes a many valued function of the time. As described previously, the generation of coalesced bubbles becomes unrecognizable after a long period, the ratio of occupation by vapour in the boiling space increases. The liquid belt which was formed continuously in a ring shape in the space is faded out, and a considerable amount of small liquid droplets adheres to the heating surface and glass tube interior. These liquid droplets move vigorously within a small range, continue to evaporate, and fade out gradually. Hereafter, the region in which the coalesced bubbles is not generated and the dry out phenomena proceeds is called the "liquid deficient region". Shift from the pre-burnout region to the liquid deficient region. and further, from the liquid deficient region to the burnout phenomenon, are smooth and slowly without interruption. It is considered that the liquid deficient region corresponds to the depressed vaporization region reported by Katto and others [9].

When the heat flux is increased further, $q > 50\,000$ kcal/m^{2}h, the heat-transfer coefficient lowers without indicating an apparent stationary value, a generation of coalesced bubbles is not recognized in the space, it enters the liquid deficient region immediately, and the dry out phenomenon proceeds rapidly on the heating surface. Thereafter, if the condition is left without taking action, it is assumed that the condition proceeds to burnout rapidly.

In the boiling within a narrow space, the time required in shifting from the pre-burnout to burnout through the liquid deficient region becomes comparatively long period under a low heat fux. However, as the heat flux increases, the required time is reduced, and under a high heat flux, the shift proceeds so rapidly that measuring procedures cannot follow the change. When observing the changes in various phenomena during such low velocity burnout more precisely and quantitatively, a hint in discovering the mechanism of burnout may be obtained. However, in this study, further detail researches and examinations were not made.

3.2 *Experiments at pressurized conditions*

When distilled water is maintained under a certain pressure and saturate-boiled within a narrow space, the boiling space indicates isolated or coalesced bubble region due to a mutual relationship between the pressure and space dimension.

3.2.1 *Behaviour of boiling.* As described above, when the space dimension is 0·57 mm and the

atmospheric-pressure water is saturate-boiled, the normal coalesced bubble range, the pre-burnout region, and the liquid deficient region appear depending on the magnitude of the heat flux, and they indicate individually different characteristics. When the space dimension is maintained constantly in 0·57 mm and the pressure inside the inner vessel is pressurized in 2 ata and 4 ata, coalesced bubbles are also generated under steady low frequency in the space. Further, on the heating surface occupied by the coalesced bubbles, existence of a thin liquid film is recognizable, and the heat-transfer characteristics of the coalesced bubble region is indicated. Figure 19 is a photograph showing an external view of the bubbles placed under pressure of 4 ata. From this photograph, it can be seen that the coalesced bubbles are being generated in the space.

When the space dimension is 0·57 mm, the pressure is 11 ata, and saturated boiling is made within the space, generation of coalesced bubbles cannot be seen although the isolated bubbles are generated in the space as illustrated in Fig. 20.

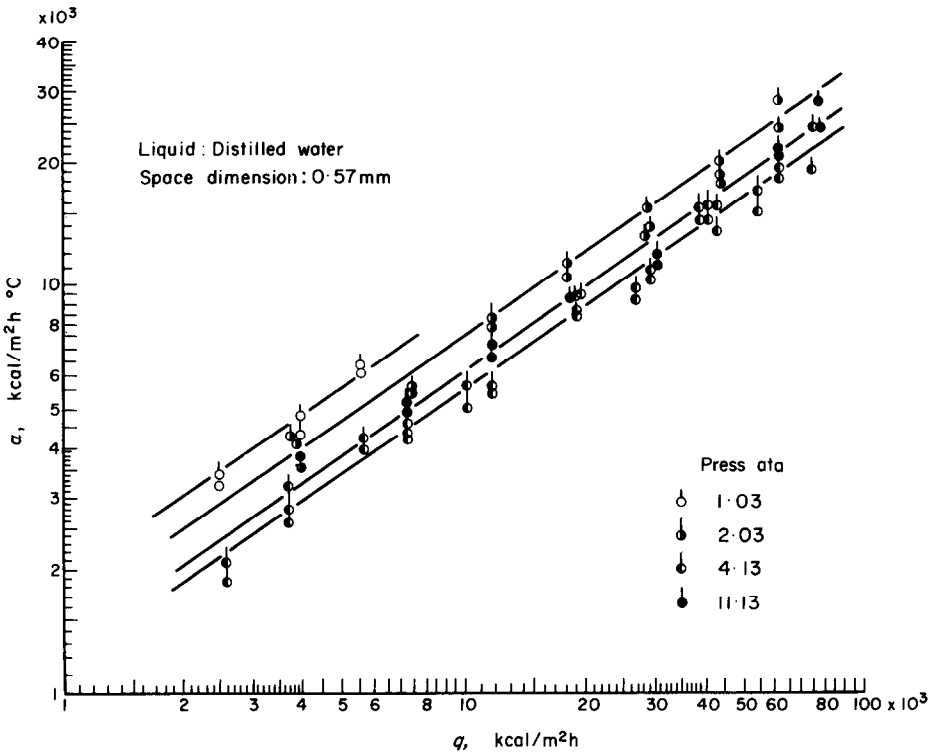

FIG. 21. Relation among heat-transfer coefficient, heat flux and pressure (distilled water, boiling space dimension at 0·57 mm).

3.2.2 *Heat transfer.* When the coalesced bubbles are generated at saturated boiling in a narrow space, similar heat-transfer characteristics are indicated, regardless of the magnitude of experimental pressure, and relation between the heat-transfer coefficient and heat flux, and relation between bubble emission frequency and the heat flux are expressed by the equations (1) and (5), respectively.

When the space dimension is 0·57 mm, the

liquid pressure is maintained constantly under 1, 2, 4, and 11 ata, and saturated boiling is carried out, the relation between the heat-transfer coefficient and the heat flux becomes as shown in Fig. 21. As described above, the ranges of pressure from 1 to 4 ata belong to the coalesced bubble region, and the higher the pressure becomes, the smaller the heat-transfer coefficient resulted at the same heat flux. It was found that the following equation can be established for relation between the pressure and heat-transfer coefficient in the coalesced bubble region at the constant heat flux.

$$\alpha \propto p^{-0.353} \tag{12}$$

When the pressure is in 11 ata, the heat-transfer coefficient contrarily increases from 4 ata. However, the reason for this is because the boundary of the coalesced bubble region and the isolated bubble region is present between 4 ata and 11 ata, and in the isolated bubble region, relation of $\alpha \propto p^{0.4}$ which has been conventionally recognized by experiments is established. The fact that the relation between heat-transfer coefficient and pressure at the coalesced bubble region becomes completely reverse to that at the isolated bubble region is a remarkable feature of the coalesced bubble region. We consider that this is related to the fact that the higher the pressure is, the more the coalesced bubble emission frequency reduces, as described below.

We also discovered that a relation between the heat flux under a pressurized condition and the coalesced bubble emission frequency is expressed by the following equation:

$$N \propto q(p\Delta R)^{-\frac{1}{2}} \tag{13}$$

To understand more generally the influence of pressure for the heat-transfer coefficient in saturated boiling within a narrow space under constant space dimension and heat flux, Fig. 22 is provided. The relation between the heat-transfer coefficient and pressure is expressed by equation (12) in the coalesced bubble region, that is, as the pressure rises the heat-transfer coefficient reduces. When the pressure increases beyond a certain value and reaches the isolated bubble region, the heat-transfer coefficient increases, and it asymptotically approaches the curve of $\alpha \propto p^{0.4}$. Contrarily, when the pressure reduces and reaches the liquid deficient region, the ratio of vapour-bubble volume occupying the narrow space increases, and as a result, the heat-transfer coefficient drops rapidly. In the boundary between these regions, no distinct

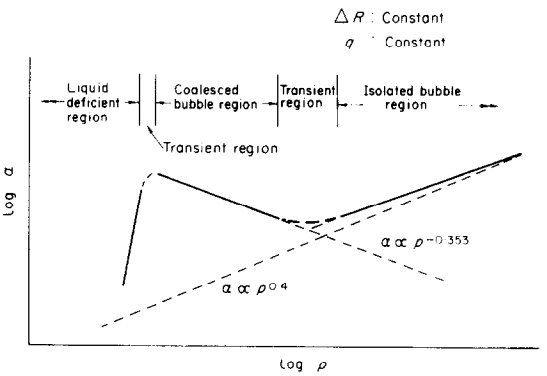

FIG. 22. Relation between heat-transfer coefficient and pressure at constant space dimension and heat flux.

boundary exists, the transient region, where both characteristics of the adjacent regions exist commonly, appears.

Moreover, in order to clarify the relations among the coalesced bubble region, isolated bubble region, and liquid deficient region more specifically, the boiling region diagram for distilled water in which the ordinate shows the pressure and the abscisa shows the space dimension is indicated in Fig. 23. The point which is plotted in this figure is lined up on the table in the same figure. However, additional tests to clarify the boundary in the coalesced bubble region and isolated bubble region are also plotted. In these tests, the space dimension and heat flux were maintained at constant values, the pressure of the inner vessel was gradually increased and decreased, thus the pressure was obtained with which change from the isolated bubble region to coalesced bubble region or

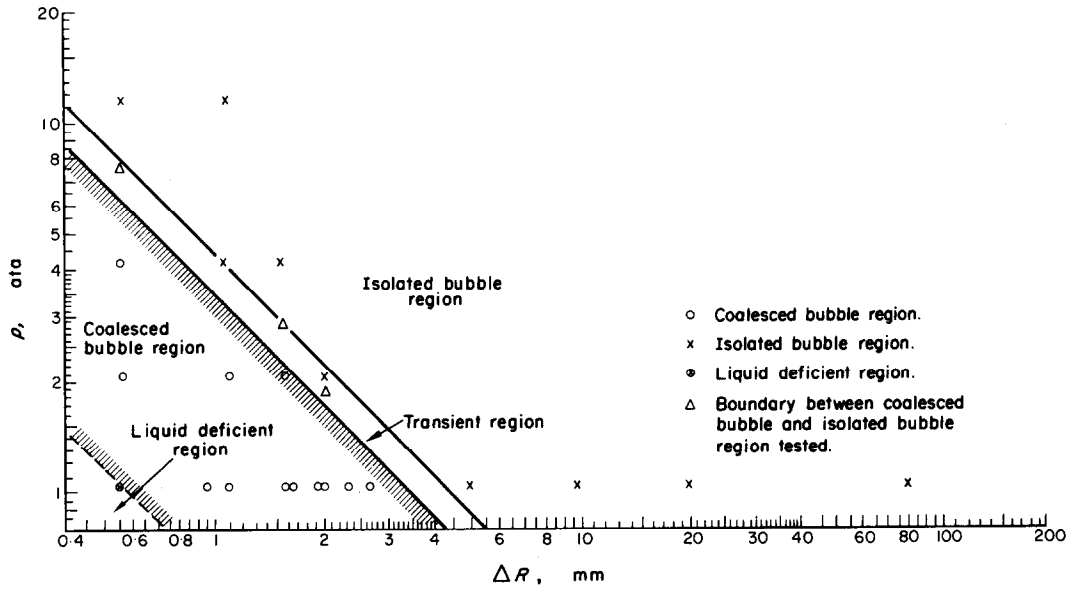

Experiment range — Figures in the table denote heat flux, kcal/m²h

Space mm / Region / Press. ata.	0·57	0·97	1·11	1·58	1·64	1·91	2·05	2·36	2·70	5·04	10·20	20·31	83·5
	Coalesced bubble region												
1	2470–79600	2300–49700	2440–76630	3860–65020	2400–47500	2400–49500	4030–65850	2300–49900	2100–57200	9400–50000	9800–56200	9300–56600	12200–49100
2	3770–64360	—	5610–76870	4080–65400	—	—	3950–60870	—	—	—	—	—	—
4	2590–76560	—	5480–76360	3670–67320	—	—	—	—	—	—	—	—	—
11	3910–79830	—	9570–62800	—	—	—	—	—	—	—	—	—	—
Boiling region	Isolated bubble region												

FIG. 23. Boiling region diagram for distilled water.

change from the coalesced bubble region to isolated bubble region is made, and the experiments were carried out for space dimensions of 0·57, 1·58 and 2·05 mm.

When the above results are summarized and the boundary line of the coalesced and isolated bubble regions are obtained, an inclined line having a slope of 45° on the ΔR axis (as shown in Fig. 23) can be drawn. In the transient region, isolated bubbles generated in the lower half of the heating surface rise along the surface within the narrow space, and then these isolated bubbles

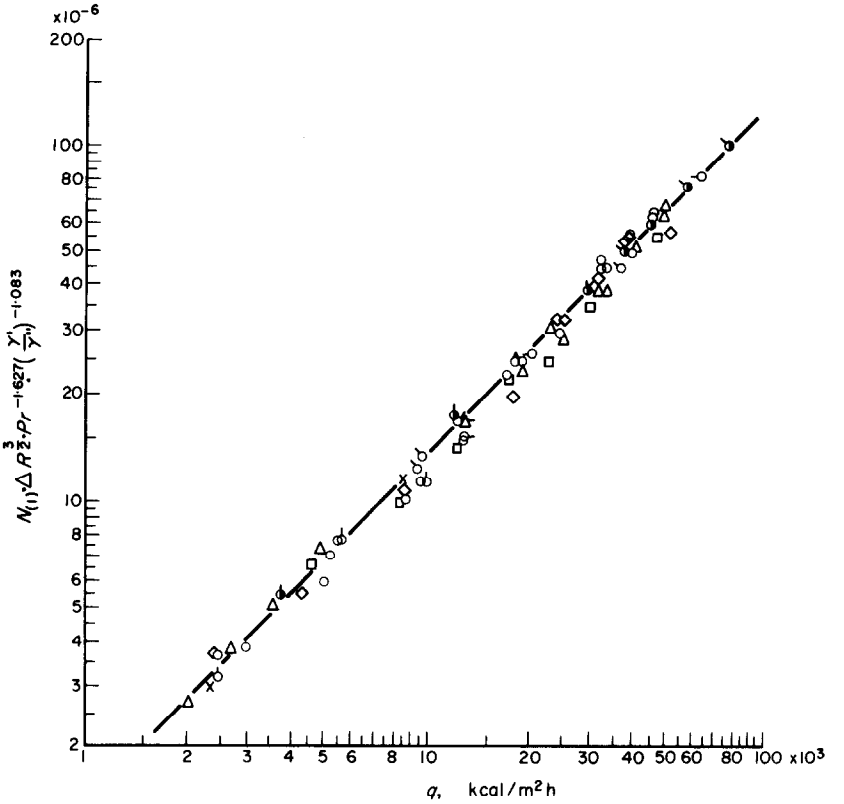

Symbol	Space mm	Press. ata	Liquid	Symbol	Space mm	Press. ata	Liquid
○	0·57	1	Distilled water	○	1·64	1	Distilled water
◑	0·57	2	Distilled water	△	1·64	1	3 ppm sodium oleate
○	1·105	1	Distilled water	◇	1·64	1	15 ppm sodium oleate
◑	1·105	2	Distilled water				
○—	1·575	1	Distilled water	○—	1·91	1	Distilled water
				△—	1·91	1	3 ppm sodium oleate
○	0·97	1	Distilled water	◇—	1·91	1	15 ppm sodium oleate
△	0·97	1	3 ppm sodium oleate				
◇	0·97	1	15 ppm sodium oleate	×	0·97	1	Ethyl alcohol
□	0·97	1	400 ppm saponin				

FIG. 24. Generalized relation between coalesced bubble emission frequency and heat flux.

grow to a coalesced bubble at the upper part of the surface. Describing the action more specifically, in this transient region also, a slight tolerance can be recognized depending on the direction of increasing or decreasing pressure, when the pressure of the test liquid is changed under a constant heat flux within the same space.

The boundary between the coalesced bubble region and liquid deficient region is indicated by one line in the figure. This is because the

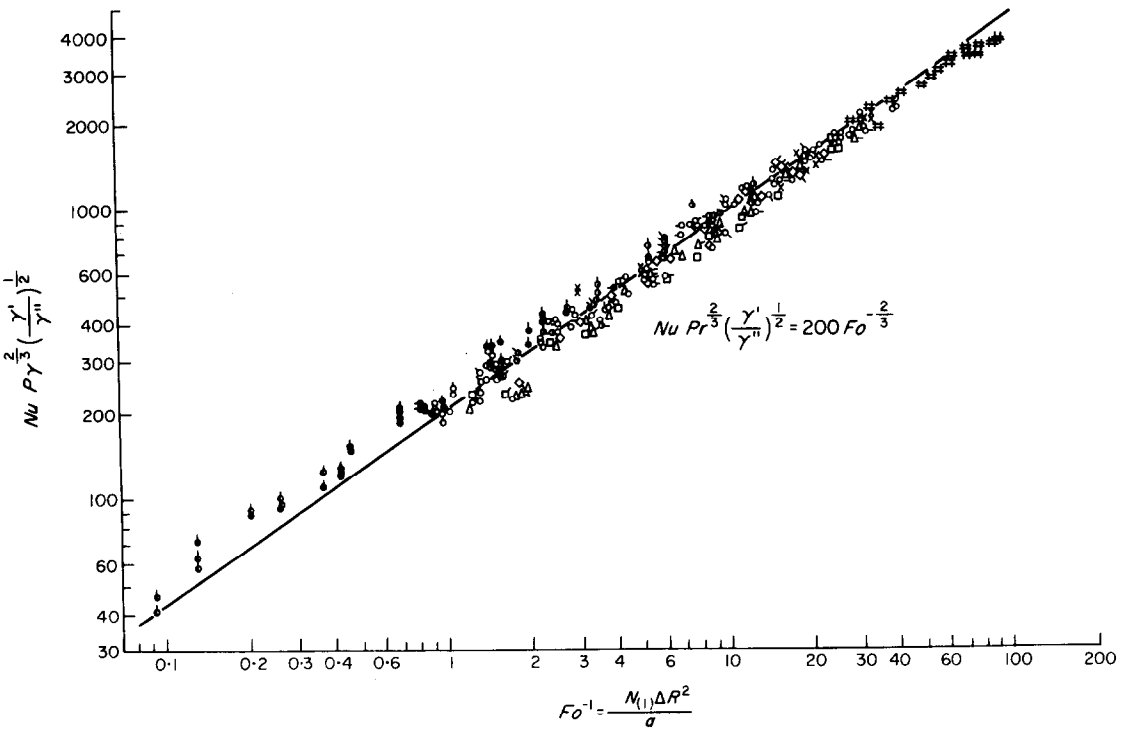

Symbol	Space mm	Press. ata	Liquid	Heating surface
○	0·97	1·03	Distilled water	80 mm dia.,
○	1·64	1·03	Distilled water	30 mm high.
○	1·91	1·03	Distilled water	Vertical
○	2·36	1·03	Distilled water	copper
○	2·70	1·03	Distilled water	cylinder.
△	0·97	1·03	3 ppm sodium oleate	
△	1·64	1·03	3 ppm sodium oleate	
△	1·91	1·03	3 ppm sodium oleate	
△	2·36	1·03	3 ppm sodium oleate	
◇	0·97	1·03	15 ppm sodium oleate	
◇	1·64	1·03	15 ppm sodium oleate	
◇	1·91	1·03	15 ppm sodium oleate	
◇	2·36	1·03	15 ppm sodium oleate	
◇	2·70	1·03	15 ppm sodium oleate	
□	0·97	1·03	400 ppm saponin	
□	1·64	1·03	400 ppm saponin	
□	1·91	1·03	400 ppm saponin	
×	0·97	1·03	Ethyl alcohol	

Symbol	Space mm	Press. ata	Liquid	Heating surface
○	0·57	1·03	Distilled water	50 mm dia.,
○	1·105	1·03	Distilled water	152 mm high.
○	1·575	1·03	Distilled water	Vertical
○	2·05	1·03	Distilled water	copper
◑	0·57	2·03	Distilled water	cylinder
◐	0·57	4·13	Distilled water	(Cr-plated).
◑	1·105	2·03	Distilled water	
◑	1·575	2·03	Distilled water	
‡	1·25	1·03	Distilled water	21·9 mm dia.,
‡	2·74	1·03	Distilled water	479 mm high.
				Vertical steel
				tube.

FIG. 25. Generalized relation of heat-transfer coefficient in coalesced bubble region by $Nu \sim Fo^{-1}$.

experiment was not conducted in detail, and we assumed that the similar transient region as described above exists. Regarding the pre-burnout, dry out phenomena, low-velocity burnout, etc., in the liquid deficient region, we did not conduct experiments in detail. When it becomes necessary to know more details, a separate study will be required.

When the coalesced bubble emission frequency obtained through the above experiments are expressed in the terms of heat flux, space dimension, and physical properties, they become as shown in Fig. 24, and the following equations are established:

$$N_{(1)} = 1{\cdot}365 \times 10^{-9} q \Delta R^{-\frac{1}{2}} Pr^{1{\cdot}627} \left(\frac{\gamma'}{\gamma''}\right)^{1{\cdot}085} \tag{14}$$

As the reader can see, almost all experimental points are within ± 10 per cent of the above equation. The applicable range of this equation is limited to normal saturated boiling of the coalesced bubble region.

Figure 25 indicates the recorrelated results of entire experimental data in this study. For the calculation of these data, the equation (14) was used for those of which the emission frequency was not measured, and when the frequency was measured, the measured value was used. As seen from this figure, all experimental data are correlated with one line, and the following equation is established:

$$Nu = 200 Fo_{(1)}^{-\frac{1}{3}} Pr^{-\frac{1}{3}} \left(\frac{\gamma'}{\gamma''}\right)^{-\frac{1}{2}} \tag{15}$$

The experimental values for atmospheric-pressure water obtained by Chernobyl'skii and Tananaiko [5] are recalculated, and plotted in the Fig. 25. The data has been properly correlated by the equation (15).

Next, for those experimental data which are considered belonging to the coalesced bubble region under experiments by Katto and Yokoya [9], the above equations (14) and (15) were applied, and we intended to correlate them. As a result, the experimental points are fitted within a range of -10–-50 per cent of equation (15), and it does not necessarily indicate a satisfactory correlation. The cause for this deviation may exist in the difference of attitude of the heating surface. More specifically, Katto and Yokoya used a horizontal copper heater having a diameter of 10 mm; however, based on the facts that no difference is recognized between experimental values for the two types of heating surface used in this study and that these values are in agreement with the experimental values by Chernobyl'skii and Tananaiko who used a completely different dimension, we consider that there is no influence from heating surface dimensions as far as the coalesced bubble region is concerned. Thus, in a horizontal surface, influence of the buoyancy force by the bubbles is weaker than that in the vertical surface, and it may be acceptable to consider that the coalesced bubble emission frequency is smaller in comparison with that of the vertical surface.

In general the saturated-boiling heat-transfer phenomena in the coalesced bubble region, the influence of the heating surface dimensions is not recognized, and it is regulated by the space dimension. However, the influence from the attitude of the heating surface cannot be disregarded. When it is desired to correlate the experimental data of the coalesced bubble region at a horizontal narrow space correctly, it is necessary to determine the constant number and reform the empirical equation separately.

Now, a description is made for liquids other than the distilled water. The heat-transfer coefficient during saturated boiling at the coalesced bubble region within a narrow space is obtained by the above-described empirical equations (14) and (15) for any desired liquid. pressure, and space dimensions. However, when these equations are applied to liquids other than the distilled water, strictly speaking, first of all, the boiling region diagram as indicated in Fig. 23 must be experimentally obtained. However, when desiring to prepare briefly a boiling region diagram without conducting an experiment, the following method may be used.

Assuming the breakoff bubble diameter during saturated boiling at standard atmospheric pressure conditions to be the maximum space dimension in the coalesced bubble region at the pressure, and this diameter is plotted on the $P - \Delta R$ diagram as shown in Fig. 23. When a straight line is drawn upward at an angle of 45° on the ΔR axis through this point, the area below this line becomes the coalesced bubble region.

4. THEORETICAL ANALYSIS

In sections 1 through 3, descriptions were presented mainly on experimental findings. In this chapter, a simple model is established in order to explain and prove heat-transfer characteristics in the coalesced bubble region, a theoretical analysis is made, and the result is described.

4.1 *Theoretical analysis* (1)

For the analysis of heat-transfer characteristics at the coalesced bubble region, the following one dimensional model is assumed. In Fig. 26, on the glass wall surface of $x = 0$,

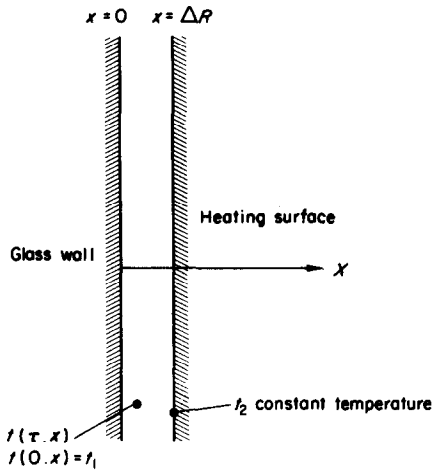

FIG. 26. Model for unsteady state thermal conduction of liquid (coalesced bubble region).

it is thermally insulated, and on the heating surface of $x = \Delta R$, it is maintained at a constant temperature t_2. The narrow space formed with the heating surface and the glass wall is filled up by a liquid at a temperature of t_1 (t_1 corresponds to saturated temperature of the liquid, moreover, it is determined that t_2 is larger than t_1) at the time $\tau = 0$, and when the $\tau = \tau$ time has elapsed, this liquid is instantaneously displaced by a coalesced bubble. It is assumed that the liquid at the temperature of t_1 is refilled up without a time delay into this empty space and this process is correctly repeated in a cyclic phase.

It is also assumed that, heat transfer is made only when the space is filled with liquid, and heat is not transferred when the space is filled with vapour. We consider that those assumptions have a sufficient propriety since thermal conductivity of the liquid is remarkably larger in comparison with that of the vapour, and the actual lodge time of the liquid is remarkably longer in comparison with that of the bubble. Further, we assume that in a narrow space, heat is transferred only by thermal conduction for the liquid. In this case, the differential equation of the thermal conduction becomes:

$$\frac{\partial t}{\partial \tau} = a\frac{\partial^2 t}{\partial x^2}, \qquad \tau > 0, \qquad \Delta R > x > 0. \tag{16}$$

The initial condition and boundary conditions for the above equation are:

$$\text{Initial condition,} \qquad t(0, x) = t_1. \tag{17}$$

$$\text{Boundary conditions,} \quad t(\tau, \Delta R) = t_2. \tag{18}$$

$$\left(\frac{\partial t}{\partial x}\right)_{x=0} = 0. \tag{19}$$

In this case, the solution is expressed by the following equation [10]:

$$t = t_1 + (t_2 - t_1) \times \left[1 - \frac{4}{\pi}\sum_{n=0}^{\infty}\frac{(-1)^n}{2n+1} \times \exp\left\{-\left[\frac{(2n+1)\pi}{2}\right]Fo\right\} \times \cos\left\{\frac{(2n+1)\pi}{2}X\right\}\right]. \tag{20}$$

Here,

$$X = \frac{x}{\Delta R}, \qquad Fo = \frac{a\tau}{\Delta R^2}. \tag{21}$$

The heat energy transferred from the heating surface to the liquid between time $\tau = 0$ to $\tau = \tau$ is expressed by the following equation:

$$q_{(0)} = \int_0^1 c\rho t\, \Delta R\, dX - \int_0^1 c\rho t_1\, \Delta R\, dX$$

$$= \Delta R c\rho (t_2 - t_1)\left[1 - \frac{8}{\pi^2}\sum_{n=0}^{\infty}\frac{1}{(2n+1)^2} \times \exp\left\{-\left[\frac{(2n+1)\pi}{2}\right]^2 Fo\right\}\right]. \tag{22}$$

Accordingly, the heat-transfer coefficient $\alpha_{(0)}$ in this case becomes:

$$\alpha_{(0)} = \frac{q_{(0)}}{(t_2 - t_1)\tau}$$

$$= \frac{\Delta R c\rho}{\tau}\left[1 - \frac{8}{\pi^2}\sum_{n=0}^{\infty}\frac{1}{(2n+1)^2} \times \exp\left\{-\left[\frac{(2n+1)\pi}{2}\right]^2 Fo\right\}\right]. \tag{23}$$

Further, when rewriting it to the Nusselt number it becomes:

$$Nu_{(0)} = \frac{\alpha_{(0)}\Delta R}{\lambda}$$

$$= \frac{1}{Fo}\left[1 - \frac{8}{\pi^2}\sum_{n=0}^{\infty}\frac{1}{(2n+1)^2} \times \exp\left\{-\left[\frac{(2n+1)\pi}{2}\right]^2 Fo\right\}\right]. \tag{24}$$

Therefore, the saturated-boiling heat transfer in the coalesced bubble region, the experimental result that the Nusselt number (used the space dimension for the representative length) can be expressed as a function of the Fourier number proved to be reasonable. Further, when equation (24) is approximated by one straight line in the range of $F_0^{-1} = 1$–40, the experimental range of this study, it becomes as shown in Fig. 27 and the following equation is established:

$$Nu_{(0)} = 0{\cdot}800\, Fo^{-\frac{2}{3}}. \tag{25}$$

4.2 *Comparison of theoretical analysis* (1) *and the results of the experiment*

Based on the one dimensional model, the theoretical solution obtained against this experimental range is equation (25). By the way, when the coalesced bubble emission frequency by thermocouple (1) is used, the empirical equation for the atmospheric-pressure water is expressed by the following equation:

$$Nu = 3{\cdot}45\, Fo_{(1)}{}^{-\frac{2}{3}}. \tag{8}$$

Equations (25) and (8) are plotted in Fig. 27. They are in agreement qualitatively but a considerable difference can be seen between them quantitatively. Hence, when equation (8) described in section 3 is used, and the Nusselt number is correlated by the coalesced bubble emission frequency at the centre and upper end of the heating surface, the following two equations are established:

$$Nu = 1{\cdot}39\, Fo_{(c)}^{-\frac{2}{3}} \tag{26}$$

$$Nu = 1{\cdot}10\, Fo_{(T)}^{-\frac{2}{3}}. \tag{27}$$

When N_1, near the lower end of the heating surface, is taken as the emission frequency, there is a considerable difference between the empirical equation Nu–$Fo_{(1)}$ and the theoretical equation $Nu_{(0)}$–Fo. However, as data at the centre and upper end of the heating surface are used for the emission frequency, this difference reduces substantially.

When examining the saturated-boiling heat transfer in the coalesced bubble region, qualitatively, an arbitrary point on the heating surface may be determined for the representative coalesced bubble emission frequency, and the frequency at this point may be used throughout the examination. However, it must be considered further, quantitatively. For the coalesced bubble emission frequency used for the cor-

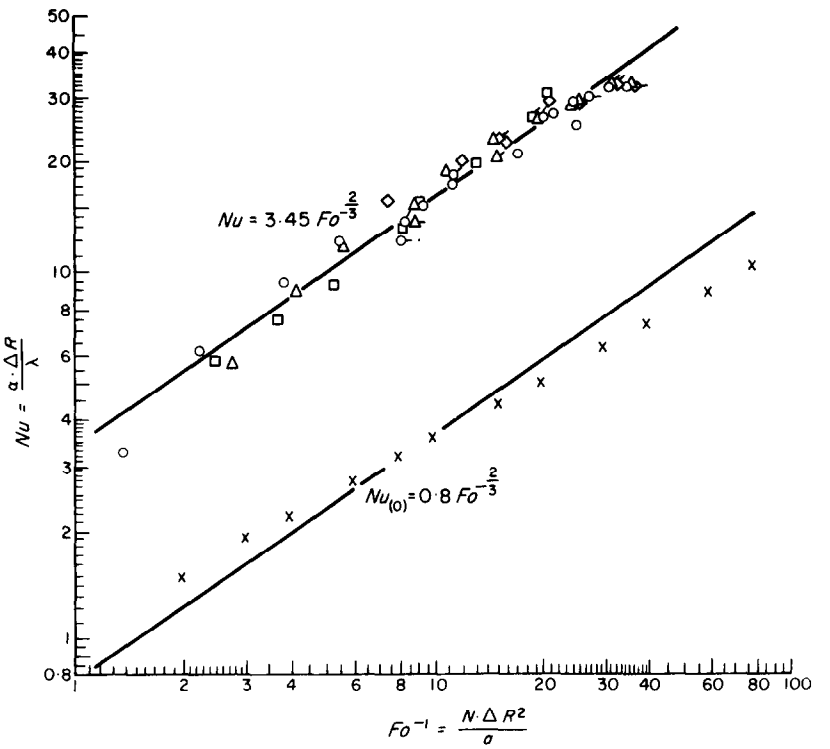

Symbol	Space mm	Press. ata	Liquid	Symbol	Space mm	Press. ata	Liquid
○	0·97	1·03	Distilled water	◇	0·97	1·03	15 ppm sodium oleate
○	1·64	1·03	Distilled water	◇	1·64	1·03	15 ppm sodium oleate
○	1·91	1·03	Distilled water	◇	1·91	1·03	15 ppm sodium oleate
△	0·97	1·03	3 ppm sodium oleate	□	0·97	1·03	400 ppm saponin
△	1·64	1·03	3 ppm sodium oleate				
△	1·91	1·03	3 ppm sodium oleate				

FIG. 27. Comparison between theoretical equation and empirical equation based on $N_{(1)}$ (atmospheric pressure water).

relation, the frequency measured by thermocouple (1), located near the lower end of the heating surface where the frequency was low, was used based on the intention to measure the frequency more accurately and also under a comparatively high heat flux range.

However, we consider that the value is improper quantitatively as the representative value because there is a considerable difference between the theoretical equation and the empirical equation as described above. Next, usage of the emission frequency at the centre of the heating surface can be considered as the representative value. However, the coalesced bubbles generated on the upper end of the heating surface affect the liquid on the heating surface as long as the liquid below them is continuous. Based on this viewpoint, usage of

the coalesced bubble emission frequency at the upper end of the heating surface may be proper.

However, when the frequency at the upper end of the heating surface (where the difference is minimized) is used, the experimental value of the Nusselt number for the same Fourier number becomes slightly larger than that of the theoretical value. Regarding this, we consider that the deviation in the above-mentioned theoretical analysis stems from the disregarding the heat transfer due to liquid rising along the heating surface and the latent heat transport due to the bubbles. Hence, by re-establishing the assumption that beside the unsteady-state thermal conduction there would be an equivalent heat source in the liquid, the following analysis is carried out.

4.3. *Theoretical analysis* (2) *and comparison with the experimental results*

When an equivalent heat source Q (kcal/m^{3}h) exists beside the unsteady-state thermal conduction, for liquid in a narrow space, the following differential equation is established:

$$\frac{\partial t}{\partial \tau} = a\frac{\partial^2 t}{\partial x^2} + \frac{Q}{c\rho}. \tag{28}$$

When the above equation is resolved for the previously described initial and boundary conditions (17), (18) and (19), the following equation is obtainable.

$$t = \frac{Q\Delta R^2 Fo}{\lambda} + t_2 + 2\sum_{n=0}^{\infty}(-1)^n \exp\left\{-\left[\frac{(2n+1)\pi}{2}\right]^2 Fo\right\} \cos\frac{(2n+1)\pi}{2} \times \left\{-\frac{Q\Delta R^2}{\lambda}\left[\frac{2}{(2n+1)\pi} \exp\left\{\left[\frac{(2n+1)\pi}{2}\right]^2 Fo\right\} \times \left\{Fo - \left[\frac{2}{(2n+1)\pi}\right]^2\right\} + \left[\frac{2}{(2n+1)\pi}\right]^3\right] - \frac{2(t_2 - t_1)}{(2n+1)\pi}\right\} \tag{29}$$

When the Nusselt number is calculated in a manner identical to the above, the equation becomes:

$$Nu_{(0)} = \frac{1}{Fo}\left\{1 - \frac{8}{\pi^2}\sum_{n=0}^{\infty}\frac{1}{(2n+1)^2} \exp\left\{-\left[\frac{(2n+1)\pi}{2}\right]^2 Fo\right\} + \frac{Q\Delta R^2}{\lambda(t_2 - t_1)}\left[\frac{1}{3} - \frac{32}{\pi^4}\sum_{n=0}^{\infty}\frac{1}{(2n+1)^4} \exp\left\{-\left[\frac{(2n+1)\pi}{2}\right]^2 Fo\right\}\right]\right\}. \tag{30}$$

In equation (30), when Q is zero, it is understood that the value agrees with equation (24). In order to eliminate the difference between empirical equation (27) and theoretical equation (25), Q is changed with equation (30) in various values, and an examination is made. Here, Q was taken at 0, 10, 20, and 30 per cent of the total heat flux, experimental values were used for the temperature difference $(t_2 - t_1)$, and the empirical equation was compared with the theoretical equation. As a result, when $Q = 30$ per cent and the emission frequency is taken at the upper end of the heating surface, the empirical equation (27) satisfactorily agrees with the theoretical equation as shown in Fig. 28.

Next, a brief consideration is made on the ratio between the total heat flux and the transferred energy by convection and latent heat transport of the bubbles. For latent heat transport of the bubbles, the bubble emission frequency becomes proportional to the heat flux, and the size of one bubble measured by a thermocouple is approximately constant regardless of the magnitude of heat flux. Thus, it may be acceptable to consider that this ratio for the total heat flow becomes approximately constant. It has already been described in section 3 that the ratio becomes slightly less than 10 per cent. Accordingly, for the convection effect, we consider that it becomes approximately 20 per cent

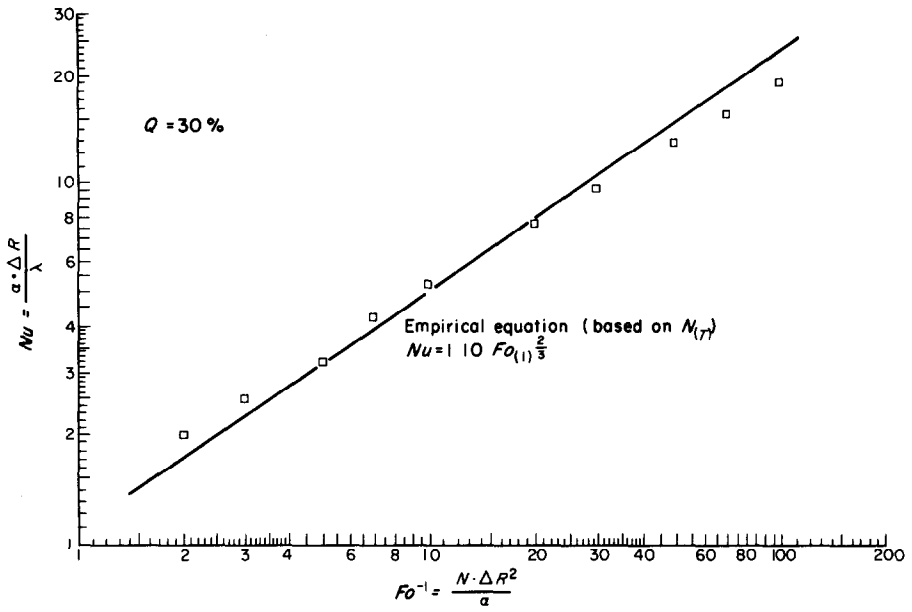

FIG. 28. Comparison between theoretical equation, considered an equivalent heat source in liquid, and empirical equation based on $N_{(T)}$ (atmospheric pressure water).

or slightly more of the total heat flow, quantitatively.

However, when an accurate value is required, more detailed experiments and theoretical studies will be required for the void ratio, rising velocities of the bubbles and velocity distribution in the liquid, and so on.

5. CONCLUSION

In this study, two vertical heating surfaces were used, and through experimental study, influence of the size of boiling space in a saturated boiling heat transfer was proved quantitatively. The boiling space dimension and pressure were changed in various values, and the regions were classified into an isolated bubble region and a coalesced bubble region, depending on whether the space dimension was larger or smaller than the critical space dimension.

In the experiments at atmospheric pressure, distilled water, water to which surface active agent was added, and alcohol were used for the test liquids. The experiments and examinations were proceeded by comparing the various characteristics of the coalesced bubble region (which were proved systematically by this study) with the various characteristics of the isolated bubble region which have been approximately systemized conventionally by many research workers. The heat-transfer coefficient in the coalesced bubble region, space dimension and heat flux are expressed by the following equation, and influence of the surface tension cannot be recognized.

$$\alpha \propto q^{\frac{1}{3}} \Delta R^{-\frac{1}{3}}.$$

For the value of heat-transfer coefficient, for example, when the space dimension is 0·97 mm, and the liquid is distilled water, it becomes approximately four times that of pool boiling. In a coalesced bubble region, the coalesced bubbles were regularly generated in a narrow space under a low frequency, and it was confirmed that the following correlating equation

was established among the heat flux, space dimension, and bubble emission frequency.

$$N \propto q\,\Delta R^{-\frac{3}{2}}.$$

In this case, also, influence of the surface tension for the coalesced bubble emission frequency is not recognized. The Fourier number based on the coalesced bubble emission frequency was introduced, and results of the atmospheric-pressure experiment were correlated. As the result, the following experimental equation was established. With this equation, experimental points in the pre-burnout region can also be correlated.

$$Nu = 4{\cdot}00\,Fo_{(1)}^{-\frac{3}{2}}\,Pr^{-0{\cdot}267}.$$

Vapour temperature within the coalesced bubbles is slightly higher than the surrounding liquid temperature, a thin liquid film existed on the heating surface of the bubble bottom, and exposure of the heating surface due to dry out of the film was recognized.

Next, with experimental apparatus for pressurized conditions, relation between pressure and heat-transfer coefficient in the coalesced bubble region was proved. Specifically, this relation is expressed by the following equation, and is completely the reverse tendency of that in the isolated bubble region.

$$\alpha \propto p^{-0{\cdot}353}.$$

For the coalesced bubble emission frequency, the establishment of the following correlating equation was recognized experimentally:

$$N \propto q\,(p\,\Delta R)^{-\frac{3}{2}}.$$

When the space dimensions were changed under a constant pressure and when pressure was changed under a constant space dimension, the experiments indicated that the following shift was carried out smoothly with a transient region having slight width, and rational correlation in these regions was proved.

(Liquid deficient region) $\rightleftarrows$ (Coalesced bubble region) $\rightleftarrows$ (Isolated bubble region).

Through this study, a correlated relation between the previously unknown coalesced bubble region (which indicates a particular bubble-generating phenomenon and heat-transfer characteristics) and the previously known isolated region was proved. The boiling region diagram was completed by correlating with these results, and the applicable limits of the correlating equation for the coalesced bubble region obtained by this study was proved.

The bubble emission frequency and heat-transfer correlating equations in the coalesced bubble region are:

$$N_{(1)} = 1{\cdot}365 \times 10^{-9} q \Delta R^{-\frac{3}{2}} Pr^{1{\cdot}627} \left(\frac{\gamma'}{\gamma''}\right)^{1{\cdot}085}$$

$$Nu = 200\,Fo_{(1)}^{-\frac{3}{2}}\,Pr^{-\frac{3}{2}}\left(\frac{\gamma'}{\gamma''}\right)^{-\frac{1}{2}}.$$

In theoretical analysis, a heat-transfer model by unsteady-state thermal conduction of liquid in a narrow space was established, a calculation was performed, and the relation of $Nu \propto Fo^{-\frac{3}{2}}$ previously obtained through the experiment was proved. For the quantitative difference between the theoretical and empirical equations, another theoretical analysis of unsteady-state thermal conduction model (to which the latent heat transport of bubble and convectional heat-transfer of liquid were considered to be a sort of heat source) was obtained, and ratio of this heat source was taken at 30 per cent of the total heat flow. The result indicated that the difference between them was eliminated and they agreed completely.

ACKNOWLEDGEMENTS

We express our deep appreciation to Professor Emeritus K. Yamagata of Kyushu University who gave us many valuable suggestions in this study. Moreover, we also express our gratitude to Mr. Akatsu of the Hitachi Laboratory who cooperated in measurements and calculation work on this study.

REFERENCES

1. K. Nishikawa, Studies on heat transfer in nucleate boiling, *Memories of Faculty of Engineering, Kyushu University* **1**, 1–28 (1956).
2. M. Jakob und W. Linke, Der Wärmeübergang beim Verdampfen von Flüssigkeiten an senkrechten und waagerechten Flachen, *Phys. Z.* **8**, 267–280 (1935).

3. E. L. PIRET and H. S. ISBIN, Natural-circulation evaporation, two-phase heat transfer, *Chem. Engng Progr.* **50**, 305–311)1954).
4. J. A. CLARK and W. M. ROHSENOW, Local boiling heat transfer to water at low Reynolds number and high pressure, *Trans. Am. Soc. mech. Engrs* **76**, 553–562 (1954).
5. I. I. CHERNOBYL'SKII and IU. M. TANANAIKO, Heat exchange during boiling of liquids in narrow annular tubes, *Soviet Phys., Technical Physics* 1244–1249 (1956).
6. N. ISSHIKI and J. TAMAKI, Considerations on boiling heat-transfer mechanism by optical observations, *J. Japan Soc. Mech. Engrs* **65**, 1393–1403 (1962).
7. *Boiling Heat Transfer J., Committee Report, Japan Soc. Engrs* 88 (1965).
8. C. Y. HAN and P. GRIFFITH, The mechanism of heat transfer in nucleate pool boiling, MIT Tech. Report No. 19 (1962).
9. Y. KATTO and S. YOKOYA, Experimental study of nucleate pool boiling in case of making interferance-plate approach to the heating surface, *Proc. 3rd Int. Heat Transfer Conf.* **3**, 219–227 (1966).
10. H. S. CARSLAW and J. C. JAEGER, *Conduction of Heat in Solid*, p. 92. Oxford University Press, London (1959).

Résumé—Dans cette étude, on signale les résultats d'une série d'expériences effectuées pour clarifier l'effet de limitation d'espace sur le transport de chaleur par ébullition saturée. Il a été découvert à partir de l'étude experimentale que dans le transport de chaleur par ébullition saturée dans un espace é troit, il y a une région à bulles en coalescence ayant des caractéristiques remarquablement différentes de la région à bulles isolées, dont les caractéristiques de transport de chaleur ont déjà été confirmées par de nombreux chercheurs. Le but principal de cette étude est de découvrir et de démontrer les caractéristiques de transport de chaleur de la région à bulles en coalescence. Dans la première moitié de l'étude, diverses caractéristiques de la région à bulles en coalescence, et celles de la région à bulles isolées sont comparées en se basant sur des découvertes expérimentales, et l'on propose en même temps un nouveau type d'équation de corrélation pour la région à bulles en coalescence. Dans la seconde moitié, on décrit une analyse théorique basée sur un modèle simple de conduction thermique en régime instationnaire et l'on démontre que l'équation de corrélation est vérifiée.

Zusammenfassung—In dieser Arbeit wird über die Ergebnisse einer Anzahl von Versuchen berichtet, die durchgeführt wurden, um den Einfluss des Blasenabstands auf den Wärmeübergang für das Sieden mit Verdampfung zu klären. Durch experimentelle Studien ist entdeckt worden, dass beim Wärmeübergang für das Sieden mit Verdampfung neben dem Gebiet der Einzelblasen ein Gebiet zusammengewachsener Blasen mit bemerkenswert verschiedenen Charakteristiken existiert, dessen Wärmeübergangskurven schon durch mehrere Forscher bestätigt wurden. Der Hauptzweck dieser Arbeit liegt in der Bestimmung und Prüfung der Wärmeübergangscharakteristiken für das Gebiet der zusammengewachsenen Blasen. In der ersten Hälfte dieser Arbeit werden die verschiedenen Charakteristiken für das Gebiet der zusammengewachsenen Blasen und das der Einzelblasen aufgrund experimenteller Ergebnisse verglichen. Gleichzeitig wird ein neuer Typ einer Gleichung für das Gebiet der zusammengewachsenen Blasen vorgeschlagen. In der zweiten Hälfte wird eine theoretische Ableitung, die sich auf ein einfaches instationäres thermisches Wärmeleitungsmodel stützt, beschrieben und die Richtigkeit der Beziehung wird nachgewiesen.

Аннотация—В статье приводятся результаты ряда экспериментов, проведенных с целью выяснения влияния ограничения пространства на теплообмен при насыщенном кипении. В результате проведенного экспериментального исследования установлено, что при теплообмене при насыщенном кипении в узком пространстве теплообменные характеристики области слияния пузырьков заметно отличаются от исследованных многими характеристик области изолированных пузырьков. Основная цель данного исследования — определить теплообменные характеристики области слияния пузырьков. В первой половине работы на основе экспериментальных данных проводится сравнение различных характеристие области слияния пузырьков и области изолированных пузырьков. Для области слияния пузырьков предложен новый тип корреляционного уравнения. Во второй половине работы проводится теоретический анализ, основанный на простой модели нестационарной теплопроводности, и дается проверка корреляционного уравнения.